JNeurosci
THE JOURNAL OF NEUROSCIENCE

Research Articles: Neurobiology of Disease

FK506-Binding Protein 12.6/1b, a negative regulator of [Ca^{2+}], rescues memory and restores genomic regulation in the hippocampus of aging rats

John C. Gant[1], Eric M. Blalock[1], Kuey-Chu Chen[1], Inga Kadish[2], Olivier Thibault[1], Nada M. Porter[1] and Philip W. Landfield[1]

[1]*Department of Pharmacology & Nutritional Sciences, University of Kentucky, Lexington, KY 40536*
[2]*Department of Cell, Developmental and Integrative Biology, University of Alabama at Birmingham, Birmingham, AL 35294*

DOI: 10.1523/JNEUROSCI.2234-17.2017

Received: 7 August 2017

Revised: 10 October 2017

Accepted: 24 November 2017

Published: 18 December 2017

Author contributions: J.C.G. and P.W.L. designed research; J.C.G., E.M.B., K.-c.C., and I.K. performed research; J.C.G., E.M.B., K.-c.C., I.K., and P.W.L. analyzed data; J.C.G., E.M.B., O.T., N.M.P., and P.W.L. wrote the paper.

Conflict of Interest: The authors declare no competing financial interests.

NIH grants AG004542, AG033649, AG052050, AG037868 and McAlpine Foundation for Neuroscience Research

Corresponding author: Philip W. Landfield, pwland@uky.edu, Department of Pharmacology & Nutritional Sciences, University of Kentucky, 800 Rose Street, UKMC MS 307, Lexington, KY 40536

Cite as: J. Neurosci ; 10.1523/JNEUROSCI.2234-17.2017

FK506-Binding Protein 12.6/1b, a negative regulator of [Ca^{2+}], rescues memory and restores genomic regulation in the hippocampus of aging rats

Abbreviated title: FKBP12.6 restores memory and genomic regulation in aging

Authors: John C. Gant[1†], Eric M. Blalock[1†], Kuey-Chu Chen[1], Inga Kadish[2], Olivier Thibault[1], Nada M. Porter[1], Philip W. Landfield[1*]

Affiliations:

[1] Department of Pharmacology & Nutritional Sciences, University of Kentucky, Lexington, KY 40536

[2] Department of Cell, Developmental and Integrative Biology, University of Alabama at Birmingham, Birmingham, AL 35294

***Corresponding author:** Philip W. Landfield, pwland@uky.edu, Department of Pharmacology & Nutritional Sciences, University of Kentucky, 800 Rose Street, UKMC MS 307, Lexington, KY 40536

† Chris Gant and Eric Blalock are co-first authors

Number of pages: 39

Number of figures: 6

Number of tables: 4

Number of words in Abstract: 249

Number of words in Introduction: 648

Number of words in Discussion: 1241

Conflict of interest: The authors declare no competing financial interests.

Acknowledgements: NIH grants AG004542, AG033649, AG052050, AG037868 and McAlpine Foundation for Neuroscience Research

Abstract

Hippocampal overexpression of FK506-binding protein 12.6/1b (FKBP1b), a negative regulator of ryanodine receptor Ca^{2+} release, reverses aging-induced memory impairment and neuronal Ca^{2+} dysregulation. Here, we test the hypothesis that FKBP1b also can protect downstream transcriptional networks from aging-induced dysregulation. We gave hippocampal microinjections of FKBP1b-expressing viral vector to male rats at either 13-months-of-age (long-term) or 19-months-of-age (short-term) and tested memory performance in the Morris water maze at 21-months-of-age. Aged rats treated short- or long-term with FKBP1b substantially outperformed age-matched vector controls and performed similarly to each other and young controls. Transcriptional profiling in the same animals identified 2342 genes whose hippocampal expression was up-/down-regulated in aged controls vs. young controls (the aging effect). Of these aging-dependent genes, 876 (37%) also showed altered expression in aged FKBP1b-treated rats compared to aged controls, with FKBP1b restoring expression of essentially all such genes (872/876, 99.5%) in the direction opposite the aging effect and closer to levels in young controls. This inverse relationship between the aging and FKBP1b effects suggests that the aging effects arise from FKBP1b deficiency. Functional category analysis revealed that genes downregulated with aging and restored by FKBP1b associated predominantly with diverse brain structure categories, including cytoskeleton, membrane channels and extracellular region. Conversely, genes upregulated with aging but not restored by FKBP1b associated primarily with glial-neuroinflammatory, ribosomal and lysosomal categories. Immunohistochemistry confirmed aging-induced rarefaction, and FKBP1b-mediated restoration, of neuronal microtubular structure. Thus, a previously-unrecognized genomic network modulating diverse brain structural processes is dysregulated by aging and restored by FKBP1b overexpression.

Significance

Previously, we found that hippocampal overexpression of FK506-binding protein 12.6/1b (FKBP1b), a negative regulator of intracellular Ca^{2+} responses, reverses both aging-related Ca^{2+} dysregulation and cognitive impairment. Here, we test whether hippocampal FKBP1b overexpression also counteracts aging changes in gene transcriptional networks. In addition to reducing memory deficits in aged rats, FKBP1b selectively counteracted aging-induced expression changes in 37% of aging-dependent genes, with cytoskeletal and extracellular structure categories highly associated with the FKBP1b-rescued genes. Our results indicate that, in parallel with cognitive processes, a novel transcriptional network coordinating brain structural organization is dysregulated with aging and restored by FKBP1b.

Introduction

Dysregulation of neuronal Ca^{2+} concentrations and of Ca^{2+}-dependent physiological responses is among the most consistent neurobiological manifestations of mammalian brain aging (Landfield and Pitler, 1984; Michaelis et al., 1984; Gibson and Peterson, 1987; Landfield, 1987; Khachaturian, 1989; Reynolds and Carlen, 1989; Thompson et al., 1996; Verkhratsky and Toescu, 1998; Hemond and Jaffe, 2005; Murchison and Griffith, 2007; Thibault et al., 2007; Oh et al., 2010). Further, Ca^{2+} dysregulation has been associated with aging-related cognitive dysfunction in multiple species (Disterhoft et al., 1996; Thibault and Landfield, 1996; Tombaugh et al., 2005; Murphy et al., 2006; Luebke and Amatrudo, 2012; Gant et al., 2015), and evidence of Ca^{2+} dysregulation also is present in postmortem Alzheimer's disease (AD) brain and in mouse models of AD (Nixon et al., 1994; Gibson et al., 1996; Stutzmann et al., 2006; Kuchibhotla et al., 2008; Overk and Masliah, 2017).

Little is known about the mechanisms underlying aging-related Ca^{2+} dysregulation, although a strong candidate mechanism, disruption of FK506-Binding Protein 12.6/1b (FKBP1b), has recently emerged. FKBP1b is a member of the FKBP family of immunophilins (Kang et al., 2008) and in muscle cells is an established negative regulator of intracellular Ca^{2+} release from ryanodine receptors (RyRs) (Zalk et al., 2007; Lehnart et al., 2008; MacMillan and McCarron, 2009).

We recently found that, in brain neurons as well, FKBP1b negatively regulates Ca^{2+} release from RyRs, and additionally, inhibits Ca^{2+} influx via membrane L-type Ca^{2+} channels (Gant et al., 2011; Gant et al., 2014; Gant et al., 2015). Selective knockdown of FKBP1b in the hippocampus of young rats recapitulates the Ca^{2+} dysregulation aging phenotype of enlarged RyR-dependent Ca^{2+} potentials and currents (Gant et al., 2011). Further, chronic stress-induced FKBP1b disruption is associated with cognitive dysfunction (Liu et al., 2012). In addition, short-term, virally-mediated overexpression of FKBP1b in rat hippocampus reverses aging-related elevation of Ca^{2+} transients and spatial memory deficits (Gant et al., 2015). Moreover, hippocampal FKBP1b expression declines with normal aging in rats (Kadish et al., 2009; Gant et al., 2015) and in early-stage AD (Blalock et al., 2004). These findings suggest FKBP1b is a key regulator of neuronal Ca^{2+} homeostasis and cognitive processing that is disrupted during aging.

Transcriptional and translational processes, notably for the activity-regulated, cytoskeletal-associated protein (Arc), also have been linked to memory, synaptic growth and dendritic remodeling (Steward et al., 1998; Guzowski et al., 2000; Schafe and LeDoux, 2000; Ploski et al., 2008; Lee and Silva, 2009; Alberini and Kandel, 2014; Fletcher et al., 2014), but it is unclear whether they are modulated by the FKBP1b network. Electrical activity at synapses and plasmalemmal membranes can trigger genomic responses via multiple Ca^{2+} signaling cascades or Ca^{2+}-dependent transcription factors (Graef et al., 1999; Gall et al., 2003; Greer and

105 Greenberg, 2008), and elevated intracellular Ca^{2+} concentrations induce electrophysiological
106 and structural signs of deterioration (Scharfman and Schwartzkroin, 1989; Bezprozvanny and
107 Mattson, 2008) that activate genomic pathways involved in cell death. Additionally, FKBP1b and
108 its protein isoform, FKBP1a, regulate non-RyR-dependent pathways, including the mechanistic
109 target of rapamycin (mTOR**)** pathway, which modulates brain-derived neurotrophic factor
110 (BDNF) and other transcriptionally active factors (Binder and Scharfman, 2004; Hoeffer et al.,
111 2008; Lynch et al., 2008). These multiple pathways of potential downstream regulation make it
112 important to determine if and how the Ca^{2+} regulator, FKBP1b, interacts with plasticity-
113 associated transcriptional processes.

114 Here, we use a multidisciplinary approach to test the hypothesis that FKBP1b overexpression
115 also counters selective aging-related alterations in transcription. In addition, to determine
116 whether long-term FKBP1b overexpression is safe and efficacious and may be a candidate
117 preventive therapy, we compare short-term hippocampal FKBP1b overexpression with long-
118 term FKBP1b overexpression, initiated in midlife when memory impairment first begins to
119 emerge (Forster and Lal, 1992; Gallagher and Rapp, 1997; Markowska, 1999; Wyss et al.,
120 2000; Bizon et al., 2009; Scheinert et al., 2015). Together, the results indicate that long-term
121 and short-term virally-mediated FKBP1b overexpression can prevent and reverse, respectively,
122 important aspects of aging-related brain decline.

123 ## Materials and Methods

124 All experiments and procedures were performed in accordance with the University of Kentucky
125 guidelines and were approved by the Animal Care and Use Committee. Hippocampal
126 overexpression of FKBP1b was induced using methods and doses similar to those we
127 described and validated previously (Gant et al., 2015). Briefly, bilateral injection of adeno-
128 associated virus (AAV) vector harboring the transgene for FKBP1b under control of the
129 calmodulin-dependent protein kinase II (CaMKII) promoter (AAV2/9.CAMKII

130 0.4.ratFkbp1b.RGB; or AAV-FKBP1b) into the CA1 region of the hippocampus. A control vector
131 harboring the transgene for enhanced green fluorescent protein (eGFP) (AAV2/9.CAMKII
132 0.4.eGFP.RGB, or, AAV-eGFP) was administered with the same procedure to a vector control
133 group of aging rats from the same cohort. The AAV vectors were constructed at the University
134 of Pennsylvania vector core (Philadelphia, PA).

135 A total of 52 male F344 rats completed behavioral training and were used for this study, divided
136 into 4 treatment groups: 1) young controls receiving no injections (YC) (n = 10, 4-5 months of
137 age at receipt) 2) Long-term aged vector control (AC) (n = 13, bilateral injections of AAV-eGFP
138 1.86e13 gene copies (GC)/mL, 2 µl per side; at 13 months-of-age; 3) Short-term FKBP1b (ST)
139 (n = 13, bilateral injections of AAV.FKBP1b 1.99e12 GC/mL, 2 µl per side, at 19 months-of-age);
140 and 4) Long-term FKBP1b (LT) (n = 16, bilateral injections of AAV-FKBP1b 1.99e12 GC/mL, 2
141 µl per side; at 13 months-of-age). All aged animals used in this study arrived together and were
142 housed in our animal care facility for the same duration. During this period, two AC, two ST
143 animals and one LT animal could not complete the study and were euthanized because of poor
144 health.

145 Infusion was accomplished using a Kopf stereotaxic instrument and Stoelting QSI microinfusion
146 pump (Stoelting Co., Wood Dale, IL). Following anesthesia, small holes were drilled bilaterally in
147 the subjects' skulls and the dura was pierced. AAV constructs were infused via 10 µl Hamilton
148 microsyringe with a 32 gauge needle (Hamilton Company, Reno, NV) into the hippocampus at a
149 rate of 0.2 µl/min. Stereotaxic coordinates were measured from bregma: 4.5 mm caudal, 3.0
150 mm lateral and depth of 1.7-1.9 mm from the brain surface based on histological pilot work.

151 The Morris Water Maze (MWM) was similar to that used in prior work (e.g., Rowe et al., 2007;
152 Latimer et al., 2014; Gant et al., 2015). Briefly, it consisted of a 190 cm diameter black round tub
153 filled with water (26° C). A 15 cm diameter escape platform was placed in one of 4 pool

quadrants 1 cm below the water. The pool was contained within a four-sided black-curtained enclosure with high contrast lighted geometric images (90 X 90 cm) on three of the curtain walls. Contrast imaging and water maze acquisition software was used for animal positional tracking and digitizing (Columbus Instruments, Columbus, OH) and measures of latency, path length to platform location and annulus crossings were recorded.

During the first 4 days (training), the escape platform remained in the same quadrant and position. Each training day consisted of three trials. On each trial, the subject was started in a different non-goal quadrant and the order of the starting quadrant was changed each day. Rats were given 60s to find the platform, and allowed to stay on the platform for an additional 30s. If the platform was not found after 60s, the rat was gently guided to the platform and allowed to stay there for an additional 30 s. On day 5 (Reference memory probe) the platform was removed and the subjects were started in the quadrant opposite the goal quadrant and allowed to swim for 60s.

On day 8, the platform was placed in a new quadrant location. The subjects were then given three trials, one from each non-goal quadrant, to learn the new platform location (Reversal training). On day 9 (Reversal memory probe) the platform was removed and subjects were allowed to swim for 60 seconds. On day 10, visual acuity and locomotor ability were assessed with the platform made visible by raising it 1 cm above the water surface and hanging a bright white contrasting marker 6 inches above the platform location. The subjects were again given three trials from each of the three non-goal quadrants to find the platform.

Three days following the visual acuity task the brains were harvested for qPCR, gene chip and immunohistochemistry studies as in prior work (Kadish et al., 2009; Searcy et al., 2012; Latimer et al., 2014; Gant et al., 2015). Animals were anesthetized with IP pentobarbital (Fatal Plus, 50 mg/kg) Following perfusion with 150 ml of cold 0.9% saline the brains were removed and

178 hemisected. For qPCR and gene chip studies the dorsal hippocampus was removed from one
179 hemisphere. This tissue was placed in RNase-free sample tubes and stored at -80° C until
180 further use. For immunohistochemistry studies, the other hemisphere was post-fixed overnight
181 in 4% paraformaldehyde, cryo-protected by submersion in 15% sucrose-PBS solution, and then
182 placed in antifreeze/30% sucrose solution for storage until sectioning.

183 Immunohistochemistry (IHC) methods were similar to those we have described previously
184 (Kadish and Van Groen, 2003; Gant et al., 2015). Coronal sections (30 μm) were cut on a
185 freezing sliding microtome. The following primary antibodies were used for overnight incubation:
186 rabbit anti-FKBP 12.6 (1:500; sc-98742, Santa Cruz, Santa Cruz, CA), and mouse MAP2
187 (1:500; MAB3418, Millipore, Temecula, CA). Following incubation, sections were rinsed and
188 transferred to the solution containing appropriate biotinylated secondary antibody for 2 hours,
189 following which they were rinsed and transferred to the solution containing ExtrAvidin for 2
190 hours. Sections were then incubated for 3 minutes with Ni-enhanced DAB solution. To obtain
191 similarly stained material, sections from all animals were stained simultaneously in the same
192 staining tray. The immunostained sections of the dorsal hippocampus were digitized using an
193 Olympus DP73 camera, and the resulting images were analyzed using ImageJ (NIH Image)
194 program. For optical densitometric analysis of MAP 2 immunohistochemistry, two sections of the
195 apical dendritic layer (stratum radiatum) of hippocampal CA1 pyramidal neurons were measured
196 per animal. Investigators were blind to animal number and condition and all photomicrographs
197 were taken with the same settings of the DP73 camera. The staining pattern of the anti-FKBP
198 12.6/1b antibody was highly similar to that seen in two prior studies of hippocampal FKBP1b
199 with this antibody, one in which we selectively knocked down FKBP1b with short hairpin RNA
200 targeting *Fkbp1b* (Gant et al, 2011), and one in which we overexpressed FKBP1b and also
201 compared endogenous FKBP1b in young vs. aged controls (Gant et al, 2015). In both prior
202 studies, the topography of FKBP1b immunostaining was highly similar to that in the present

study and the antibody clearly detected the experimental manipulations and the aging difference in FKBP1b expression in CA1. In addition, the vendor validates antibody specificity by western blot analyses, and we performed negative control studies by omitting the primary antibody and using only secondary in adjacent brain sections from the same subjects. These negative controls produced no staining in our rat brain tissues.

Dorsal hippocampal RNA was extracted according to standard protocols, and evaluated using Agilent Bioanalyzer. All samples were of sufficient quality and did not differ significantly among treatment groups (RNA Integrity Number [RIN]: 9.4 ± 0.1 for all groups; $p = 0.16$, ANOVA across YC, AC, ST and LT groups). Extracted RNA was used for both PCR and microarray measures. For RT-PCR mRNA quantification, one-step real-time reverse transcription PCR (qRT-PCR) was utilized. RT-PCR amplification was performed as described previously (Gant et al., 2015) using an ABI prism 7700 sequence detection system (Applied Biosystems, CA, USA) and RNA-to-CT 1-step TaqMan kit (Life Technologies, MA). All samples were run in duplicate in a final volume of 30 µl containing 25-50 ng of cellular RNA and a Taqman Fam-MGB probe (Rn00575368_m1, Life Technologies) with an amplicon spanning 116 bp rat FKBP1b cDNA region. Cycling parameters for all assays were as follows: 30 min at 48°C, 10 min at 95°C followed by 40 cycles of 15 sec at 95°C and 1 min at 60°C. The RNA levels of glyceraldehyde-3-phosphate dehydrogenase (Gapdh) were used as normalization controls for RNA quantification.

Microarray procedures were similar to those in our prior microarray studies on hippocampal aging in rats (Blalock et al., 2003; Rowe et al., 2007; Kadish et al., 2009). Briefly, RNA extracted from dorsal hippocampus was labeled and hybridized to Affymetrix Rat Gene 1.0 ST arrays (one array per animal). Gene signal intensities for microarrays were calculated using the Robust

Multi-array Average (RMA) algorithm (Bolstad et al., 2003) at the transcript level and data were associated with vendor-provided annotation information.

Experimental design and statistical analyses (Fig. 1). To test the hypothesis that expression in selective genomic systems parallels the changes in memory performance induced by aging and, in the opposite direction, by FKBP1b rescue, we compared young adult control (YC) rats and aged vector control (AC) rats (that received bilateral injections of AAV-eGFP) with aged rats that received bilateral dorsal hippocampal injections of AAV-FKBP1b. The FKBP1b expressing virus was microinjected into aging rats either 2 months (short term: ST) or 8 months (long term: LT) prior to testing spatial reference and reversal learning in the Morris Water Maze (MWM). All three aged groups were tested together at 21 months of age along with young (5 month old) controls (Fig. 1). The reference memory task tests the ability to learn an aspect of the task that remains constant, whereas reversal learning comprises elements of both working memory and executive cognitive function (Webster et al., 2014) and is well-recognized to be particularly susceptible to impairment with aging (Bartus et al., 1979; Stephens et al., 1985). Initial statistical assessments of behavioral comparisons used analysis of variance (ANOVA). If significance was found at the ANOVA level (α = 0.05), then protected Fisher's Least Significant Difference (pLSD) pairwise contrasts (α = 0.05) between groups were also performed.

Microarray profiling was undertaken with the goal of identifying the FKBP1b-sensitive transcriptome. The n's chosen for microarray studies were based on our prior work (Blalock et al., 2003; Rowe et al., 2007; Kadish et al., 2009; Blalock et al., 2010), which found that n's of 5-10 per group are sufficient to consistently identify a distinct hippocampal aging transcriptome. For transcriptional profiling in the present study, a sub-group of 6 subjects was selected from each of the four parent treatment groups (N=24 rats, one array per rat). To reduce false negatives and maximize the transcriptional responses to elevated FKBP1b expression, we selected subjects for the ST and LT sub-groups that showed *Fkbp1b* expression levels above

the medians for the parent groups. The YC and AC groups exhibited low within-group variance of *Fkbp1b* expression (Fig. 3) and these sub-groups were selected at random from within their parent groups.

The Rat Gene Array used for the microarray analysis contains 29,218 total probe sets, which we filtered prior to statistical testing to retain only the 14,828 probe sets characterized by unique gene annotations and by signal intensity (expression) adequate to show presence of the gene (defined as unlogged signal intensity ≥ 40 on ≥ 4 arrays in the study.). Expression of each of these 14,828 genes was tested by one-way ANOVA to identify genes exhibiting significant differences in expression across the four groups. Outlier values (> 2 SD of the group mean) were treated as missing values. Transcriptional profiling analyses can involve thousands of statistical comparisons and consequently, require assessment of multiple testing error. We estimated the error contributed by multiple testing using the False Discovery Rate (FDR) procedure (Hochberg and Benjamini, 1990). The FDR is the ratio of significant comparisons expected by chance to significant comparisons actually observed. The FDR is an estimate of the probability that any single significant gene in a profiling study is a false positive found due to the error of multiple testing. Therefore, confidence in profiling data increases as the FDR decreases. Confidence in microarray data is also strengthened considerably by functional category analyses, which can determine whether multiple genes in the same functional categories are co-regulated (Blalock et al., 2005; Ginsberg and Mirnics, 2006).

For functional category analysis in the present study, ANOVA-significant genes were assigned to one of four expression template patterns defined by post hoc pairwise comparisons between groups (see Results). Overrepresented functional categories for each expression template were determined using Database for Annotation, Visualization and Integrated Discovery (DAVID) bioinformatic tools (Huang et al., 2009) with the list of 14,828 filtered genes as a background. Raw data are available through the Gene Expression Omnibus (GSE #: 102054).

To determine the functional categories/pathways which were closely associated with each of the four template patterns, functional pathway analysis was performed as in prior work (Blalock et al., 2003; Blalock et al., 2004; Rowe et al., 2007; Kadish et al., 2009; Chen et al., 2013). Genes assigned to each of the four template patterns were statistically tested (α = 0.05) using a modified Fisher's exact test p-value referred to as the 'Ease score' in the DAVID suite of bioinformatic tools (Huang et al., 2007). This approach was used to test the Gene Ontology database (biological process, cellular component, molecular function) for categories overrepresented by genes of each template pattern. Medium classification stringency was applied. Functional annotation clustering output from DAVID was transferred to flat files, and the most significant annotation from within each cluster was identified. Among these, unique functional annotations with significant Ease scores are reported along with the number of associated pathway genes.

In a further assessment of possible contributions of chance to these large-scale analyses, the numbers of genes that were identified as belonging to a particular pattern were compared with the numbers of genes that would be expected to fall within that pattern by chance. The probability that a gene would fall into a particular pattern by chance was estimated by performing a Monte Carlo analysis, in which the same statistical procedures (ANOVA test, post hoc pLSD and template pattern) and statistical criteria (α = 0.05) are used, but applied to random numbers, rather than actual gene signal intensity values. The Monte Carlo procedure was re-run 1000 times, with a newly generated set of random numbers in each iteration. The average number of genes found to fall within each expression pattern across 1000 iterations of random data was then used as an estimate of the number of genes expected to fall within that pattern by chance. The binomial test (α = 0.05) was used to determine whether the number actually found in the pattern significantly exceeded the number expected by chance.

Results

FKBP1b overexpression improved spatial reference and reversal memory for both LT and ST aged groups (Fig. 2).

A total of 52 rats in 4 groups completed our spatial memory testing protocol in the MWM (10 YC, 13 AC, 13 ST and 16 LT rats). For the 3 groups of aged AAV-treated rats, behavioral testing began at 21 months of age, either 8 (long-term) or 2 (short-term) months following AAV injection. Training in the MWM reference memory task was performed over 4 days, with 3 training trials per day. Over the 4 days, all groups showed acquisition of the task as indicated by a distinct decline in latency and path-length to find the platform ($F_{11, 528}$ = 11.58 p =1.80e-10; $F_{11, 528}$ = 7.41, p = 7.20e-12, respectively, repeated measures ANOVA). Although there was a strong trend for young animals to outperform aged controls during training, no significant effects of treatment were seen in latency and path length measures over this 4-day training phase, similar to results in Gant et al (2015).

On the 5th day of the task, the platform was removed and recall of the platform location was probed with a single retention trial (Fig. 2A; Reference Memory Probe). There was a main effect of treatment group for both latency ($F_{3, 48}$ = 3.57, p = 0.021, ANOVA) and path length ($F_{3, 48}$ = 2.90, p = 0.044, ANOVA). As reported in multiple studies, Aged Controls exhibited significantly longer path lengths and higher latencies to find the platform compared to Young Control rats. In contrast, neither FKBP1b-treated aged group differed from YC and both showed significantly reduced latency compared to Aged Controls (vs. AC: LT, p = 0.05, ST, p = 0.05; YC, p =0.002, pLSD). The path length to platform results were highly similar to latency although the differences between the FKBP1b groups and the Aged Controls were only of borderline significance (vs. AC: LT, p = 0.078; ST, p = 0.08, YC, p = 0.006, pLSD).

Training on the Reversal Memory task was conducted on the 8th day, following two days of rest: The location of the platform was changed and the rats were given 3 trials in one day to learn the new location. Over the 3 reversal training trials, there were no significant differences in latency or path length among any of the groups nor was there significant improvement (data not shown). On the 9th day, the platform was again removed and rats were tested for their retention of the new platform location on a single retention trial (Fig. 2B, Reversal Memory Probe). There were substantial main effects of treatment on latency to platform ($F_{3, 48}$ = 9.57, p = 0.000046, ANOVA) and path length to platform location ($F_{3, 48}$ = 7.97, p = 0.0002, ANOVA). Aged control animals again exhibited highly significant deficits in path length and latency compared to young controls, but both ST and LT groups exhibited path length and latency scores tha7t were highly similar to those of YCs and significantly reduced compared to AC animals (latency; AC vs: LT, p < 0.0001, ST, p < 0.0001; YC, p < 0.0001; path length, AC vs: LT, p = 0.0001, ST, p = 0.0001; YC, p =0.0008, pLSD) (Fig. 2B). There was also a main effect of treatment group for platform crossings during the reversal retention test ($F_{3, 48}$ = 7.37, p = 0.0004; ANOVA), with the YC, ST, and LT groups showing significantly greater platform crossings compared to AC (AC vs: YC, p < 0.0001; ST; p < 0.025; LT, p < 0.01, pLSD).

On the 10th day of the protocol, a cued retention test was given with visual cues highlighting the platform's location. All groups found the platform rapidly and no significant group differences were present in latency, path length or swim speed in locating the platform (Fig. 2C, Cued Trial), indicating that aging-related changes in locomotor and visual acuity did not account for the differences in memory performance.

Notably, the ST and LT groups were statistically indistinguishable from each other on all latency and path length measures in the behavioral testing protocols. These results suggest that the reversal by ST and prevention by LT of aging-dependent memory impairment may be mediated by similar cellular mechanisms despite the differences in the duration of exposure.

AAV-FKBP1b injection increased hippocampal FKBP1b expression, particularly in the long-term group (Fig. 3).

Because the Affymetrix Rat Gene 1.0 ST microarray used in the present study does not include the probe set for *Fkbp1b*, we used qRT-PCR to evaluate the effectiveness of AAV-FKBP1b injection for inducing FKBP1b expression in hippocampus. *Fkbp1b/ Gapdh* expression is plotted as a function of treatment group (Fig. 3). There was a highly significant increase in *Fkbp1b* expression ($F_{3, 47}$ = 18.449, p = 0.000050, ANOVA on ranks (Kruskal Wallis)). By pairwise contrast (Fisher's LSD on ranks), the increased expression was significant in ST (p = 0.012), and highly significant in LT (p < 0.001). Immunohistochemistry in representative animals indicated that hippocampal FKBP1b protein upregulation paralleled *Fkbp1b* mRNA increases in AAV-FKBP1b-treated rats, and was particularly intense in LT animals (Fig. 3, lower).

In contrast to our prior findings (Blalock et al., 2004; Kadish et al., 2009; Gant et al., 2015), we did not observe differences in endogenous FKBP1b expression between Aged and Young Control groups (Fig. 3, upper). This may be due to differences between studies in tissue dissection. In the present study we collected tissue from whole dorsal hippocampus, whereas in prior work we measured expression primarily in the CA1 region (Blalock et al., 2004; Kadish et al., 2009; Gant et al., 2015). Therefore, the aging effect on FKBP1b in CA1 might have been obscured in the present work because of dilution from less age-sensitive hippocampal regions. Further studies will be needed to fully elucidate the topographic distribution of aging changes in FKBP1b expression as well as the role of potential functional changes (e.g, Lehnart et al., 2008).

Transcriptional profiling (Fig. 4).

To identify genes whose expression paralleled aging and FKBP1b's cognitive effects in the same animals, we first distinguished genes that changed expression with aging (i.e., differed

between AC and YC, the aging effect). We then identified those genes among the aging-dependent genes that were also altered by FKBP1b overexpression (i.e., differed between LT/ST FKBP1b and AC, the FKBP1b effect). RNA from 6 subjects per treatment group was prepared and hybridized to Affymetrix Rat Gene 1.0 arrays. Of the ~30,000 probe sets on the array, we filtered to retain 14,828 annotated, present genes (see Methods) for statistical analysis. One-way analysis of variance (ANOVA; $p \leq 0.05$) showed that 24% (3,502) differed significantly across the 4 groups, yielding a False Discovery Rate (FDR) = 0.12 (see Methods). An FDR of 0.12 is quite low for a microarray study of brain aging and provides considerable confidence in these results. As noted, reliability in microarray studies is also strengthened when functional categories are overrepresented by co-regulated genes (Blalock et al., 2005; Galvin and Ginsberg, 2005; Ginsberg and Mirnics, 2006).

Among ANOVA-significant genes (3,502), 2,342 (67%) also differed significantly in pairwise contrast (Fisher's protected Least Significant Difference; $p \leq 0.05$) between the Young and Aged Control groups (aging-dependent genes, 'the aging effect'). Among these, the expression levels of 37% (876/ 2,342) genes were also altered by FKBP1b overexpression (517 by LT, 193 by ST, 166 by both ST and LT, 'the FKBP1b effect') and were defined as aging and FKBP1b-sensitive genes (See extended data Fig. 4-1 for a complete list of aging- and FKBP1b-sensitive genes). Many more of these were altered by both ST and LT (166) than would be expected by chance if ST and LT treatments acted through independent mechanisms ($p = 4.8E\text{-}9$, binomial test). These results suggest that LT and ST FKBP1b treatments exerted similar transcriptional effects. To determine whether this agreement between ST and LT was limited primarily to the 166 genes in the overlap, or instead reflected widespread similarity among most FKBP1b-sensitive genes, we tested the correlation between LT and ST effects across all 876 FKBP1b-sensitive genes. A highly significant proportion of FKBP1b-sensitive genes (822/ 876; 93.8%) were changed in the same direction by both ST and LT ($p \leq 1E\text{-}12$, binomial test). Further, the effect

399 sizes of ST and LT treatments genes (expressed as log2 fold-change vs. Aged Control) were
400 strongly correlated (R = 0.85, p = 1.3E-24; Pearson's test, data not shown). These results
401 indicate that ST and LT FKBP1b treatments influenced gene expression similarly. As noted, the
402 ST and LT groups also performed nearly identically on all behavioral measures. Based on these
403 similarities and because the Genome Ontology functional category analysis (see below)
404 provides greater statistical confidence in overrepresentation of a given category with increasing
405 numbers of genes assigned to that functional category, we combined the ST and LT lists of
406 FKBP1b-sensitive genes into a single list, such that a gene was considered an FKBP1b-
407 sensitive gene if it differed from aged controls with ST and/ or LT treatment.

408 Remarkably, only 4 of the 876 aging-dependent and FKBP1b-sensitive genes (Eif3g, Pla2g7,
409 S100b, and Snapc2) exhibited exacerbation of aging effects by FKBP1b, whereas the other 872
410 changed in opposite directions with aging and FKBP1b treatment. Accordingly, the anomalous 4
411 genes were excluded from functional category analyses and the remaining aging-dependent
412 genes (2338) were parsed into one of four gene expression templates (Fig. 4, right, I-IV), which
413 reflected direction of a gene's expression change with aging (up or down) and whether the gene
414 did (Fig. 4, templates II and IV), or did not (Fig. 4, templates I and III) show the coucnteracting
415 effect of FKBP1b treatment (LT or ST vs. AC; $p \leq 0.05$, Fisher's post-hoc Least Significant
416 Difference).

417 To determine whether the number of genes identified in each template was greater than
418 expected by chance, we ran a Monte Carlo simulation using the same statistical analysis and
419 template assignment strategy, but with randomly generated numbers substituted for signal
420 intensity values (see Methods). The numbers of genes actually observed for each reported
421 pattern exceeded by > 11 fold the number expected by chance based on the simulation (Fig. 4)

422 (≤ 0.00001, binomial test for each pattern), indicating a strong biological effect.

Gene Ontology (GO) functional categories associated with genes matching each of the four template patterns (Fig. 4) of Aging- and FKBP1b-sensitive genes (Table 1).

Lists of genes assigned to each of the four expression templates described above (Fig. 4) were separately uploaded to DAVID (Huang et al., 2007) and the Biological Process, Cellular Component, and Molecular Function Gene Ontologies were interrogated. In each significant cluster, the most statistically overrepresented functional category (by DAVID Analysis) with more than 3 genes was retained. The retained functional categories for each of the 4 templates are shown in Table 1 (and individual genes associated with each identified functional pathway are listed in extended data Table 1-1).

Genes downregulated-with-aging and unchanged by FKBP1b (AC down vs. YC, template I) overrepresented GO annotations associated with neurotransmitter metabolism and biosynthesis in neurons. Their downregulation with aging may reflect a reduction of neuronal growth and synthetic processes.

Genes upregulated-with-aging and unchanged by FKBP1b (AC up vs. YC, template III) very strongly overrepresented functional categories associated with upregulated translational elongation, lysosome activity, and immune signaling, which appear to reflect major turnover of proteins, cholesterol transport and new biosynthesis of apolipoproteins by astrocytes as well as activated neuroinflammatory signaling by microglia. Similar patterns have been seen in multiple studies, (Weindruch and Prolla, 2002; Blalock et al., 2003; Rowe et al., 2007; Kadish et al., 2009; VanGuilder et al., 2011; Chen et al., 2013). Surprisingly, inflammatory responses have generally not been found to correlate closely with learning or memory (Rowe et al., 2007; Kadish et al., 2009; VanGuilder et al., 2011), and their resistance to counteraction by FKBP1b, seen here, extends those prior findings.

Genes downregulated-with-aging, upregulated-by-FKBP1b (AC down vs. YC, FKBP1b up vs. AC, template II) strongly overrepresented GO categories related to intracellular and extracellular structure, including: cytoskeleton; extracellular region, passive transmembrane transporter activity; ectoderm development; regulation of actin cytoskeleton organization and regulation of MAP kinase activity (Table 1), as considered further in Discussion.

Genes upregulated-with-aging, downregulated-by-FKBP1b (AC up vs. YC, FKBP1b down vs. AC, template IV) overrepresented GO category annotations related to extracellular remodeling and transporter activity, including extracellular matrix, primary transmembrane transporter activity, blood vessel development, regulation of cell motion and membrane-bounded vesicle (Table 1), potentially reflecting extracellular reorganization, glial and endothelial cell cytokinesis and transport of substances between activated cells.

Microtubule Associated Protein-2 (MAP2): downregulation with aging and restoration by FKBP1b (Fig. 5).

The 'cytoskeleton' category was the most statistically significant downregulated-with-aging upregulated-by-FKBP1b functional category, and has been consistently identified as age-dependent in our prior studies on hippocampal gene expression associations with memory (Blalock et al., 2003; Rowe et al., 2007; Kadish et al., 2009). Accordingly, to confirm that these gene expression alterations were reflected in cytoskeletal changes at the protein level, we used semi-quantitative immunohistochemistry to analyze MAP2, an abundant somatodendritic microtubule associated protein that reflects general microtubular structure. (Fig. 5). MAP2 protein expression was significantly reduced ($F_{3, 18}$ = 7.792, p = 0.0015, ANOVA, ** post-hoc pLSD $p \leq 0.001$) with age and rescued by LT treatment (pLSD $p \leq 0.01$) and possibly ST treatments (borderline significant, pLSD p = 0.06), consistent with the view that the cytoskeletal genomic alterations are reflected in overall function and protein structure of the cytoskeleton.

Possible downstream mediators of FKBP1b effects.

Calpain-1, calcineurin and other Ca^{2+}-related genes (Table 3). Because FKBP1b is a negative regulator of hippocampal neuronal Ca^{2+} transients (Gant et al., 2011; Gant et al., 2015) it seemed feasible that pathological Ca^{2+}-related signaling during aging might be restored to young levels by FKBP1b overexpression. We therefore identified all Ca^{2+}-related genes on the microarray and determined which showed age-related changes in gene expression that were significantly countered by FKBP1b treatment (i.e., met the criteria for template II or IV in Fig. 4). Although Ca^{2+}-related genes as a category did not show significant overrepresentation of genes whose aging changes were countered by FKBP1b, two Ca^{2+}-sensitive enzymes frequently associated with brain aging, neuronal plasticity and Alzheimer's disease (calpain-1 and calcineurin, Nixon et al., 1994; Rozkalne et al., 2011; Furman and Norris, 2014), as well as a Ca^{2+} release-activated Ca^{2+} channel (ORAI1) were altered by aging and restored by FKBP1b treatment (Table 3). These Ca^{2+}-related genes, therefore, may be sensitive downstream mediators of some aspects of both age-dependent neuronal Ca^{2+} dyshomeostasis and restoration of regulation by overexpression of FKBP1b.

mTOR pathway genes. Genes in the mechanistic target of rapamycin (mTOR) pathway were also of specific interest, as this pathway is inhibited by the immunosuppressant drug rapamycin via complex formation with FKBP1b/1a. Moreover, FKBP1a, a close isoform of FKBP1b, negatively regulates mTOR in brain, even in the absence of rapamycin (Hoeffer et al., 2008). These interactions of FKBPs and mTOR appear to occur independently of FKBP1b/1a-dependent regulation of Ca^{2+} release from RyRs. Therefore, to determine whether mTOR pathway expression is altered by FKBP1b activity, we investigated mTOR pathway gene expression relative to FKBP1b overexpression. Twenty-four mTOR pathway genes were identified by searching the Gene Ontology database as well as the literature (e.g., Johnson et al., 2013). Of these 24, only two, Hif1an and Nfkb1, were significantly altered with both age

(upregulated) and FKBP1b (downregulated), showing that the mTOR pathway was not statistically overrepresented by FKBP1b-sensitive genes (n.s., p = 0.78, binomial test). Protein-protein interactions importantly regulate mTOR signaling. Nevertheless, the lack of change in mTOR pathway gene expression suggests that FKBP1b's genomic effects were not mediated by the mTOR pathway.

Discussion

The present studies provide the first evidence that FKBP1b, a negative regulator of intracellular [Ca^{2+}], modulates a previously-unrecognized genomic network regulating structural organization of the brain. In the hippocampus this network appears to be specifically targeted and dysregulated by aging. However, as shown here, FKBP1b overexpression can largely reverse or prevent aging-dependent alterations in gene expression in the network. In this study, FKBP1b overexpression restored regulation of this network in parallel with cognitive rescue in the same aged rats. Thus, this genomic evidence adds strong new support for the hypothesis that FKBP1b is a linchpin of neuronal homeostasis that functions at multiple levels, including regulation of Ca^{2+}, maintenance of structural integrity and preservation of cognitive function.

Aging-induced changes in gene expression

As in our prior work, we found a high proportion of hippocampal genes (2342/14,928) significantly altered with aging (Fig. 4- the 'aging effect'). Further, the expression levels of 37% of these aging-altered genes also differed significantly between aged control and aged FKBP1b rats (876/2,342 genes- the 'FKBP1b effect'). Regardless of whether the aging effect for a given gene was up- or down-regulation, FKBP1b shifted the expression levels for essentially all of these genes (872 of 876, 99.5%) back toward their young control levels. This remarkably consistent restorative action of FKBP1b strongly suggests that disruption of FKBP1b, or closely

associated molecules, may underlie a significant portion of the aging effect for the 872 FKBP1b-regulated genes.

Nevertheless, deficient FKBP1b function does not account for all aspects of genomic change with brain aging. Of the aging-altered genes, a majority (1462/2342, ~63%) were not affected by FKBP1b overexpression. Notably, those associated with upregulated glial-inflammatory processes were unaffected by FKPB1b (Table 1). Consequently, it appears that other aging processes (e.g., glial) also modulate hippocampal transcription, but operate independently from, or upstream of, the FKBP1b-sensitive genomic network.

FKBP1b overexpression reveals an apparent genomic network that regulates neuronal structure and is targeted by aging

FKBP1b-restored genes were predominantly associated with GO functional categories related to diverse components of brain structure. In particular, *cytoskeleton*, *passive membrane transport* (ion channel proteins that add structure to lipid bilayer membranes) and *extracellular region* were the three functional categories most overrepresented by genes whose expression declined with aging and increased with FKBP1b (Table 1). The *cytoskeleton* category was represented by numerous genes related to actin, intermediate filaments and microtubule assembly, whereas the extracellular region category was represented by multiple genes encoding collagens and matrix metalloproteinases, two families essential for extracellular matrix assembly/remodeling. Similarly, among genes whose expression increased with aging and declined with FKBP1b, the most overrepresented category was *extracellular matrix*, which, despite also focusing on extracellular space, was represented by a markedly different group of genes. The *extracellular matrix* category included genes encoding proteoglycans, growth factors and other proteins associated with glial activation and blood vessel development (Table 1 and extended data Table1-1). These patterns of expression in FKBP1b-sensitive aging genes

appear to reflect an aging-related shift in biosynthetic activity and differentiation from neuronal and extracellular structure to glial processes/compartments. Together, the disparate structural 0systems altered by aging and restored by FKBP1b suggest the operation of a novel genomic network that coordinates structural assembly among diverse brain components. This network is particularly targeted by aging but the disruptive effects of aging can, as shown here, be prevented or reversed by FKBP1b overexpression in neurons.

It seems of considerable interest that cytoskeletal remodeling in dendritic spines has been s0hown to play a critical role in long-term potentiation (Lynch and Baudry, 1987; Lynch et al., 2008; Briz and Baudry, 2016). In the present study, cytoskeletal gene downregulation with aging and protection by FKBP1b was among the major effects and was confirmed at the protein level by IHC analyses of MAP2, the primary microtubule associated protein of somatodendritic compartments (Fig. 5). However, more than one FKBP1b-associated process likely participates in memory formation. Accordingly, defining the precise pathways linking FKBP1b ov0erexpression to counteraction of age-related memory decline will require substantial further study.

The gene encoding calpain-1, a major Ca^{2+}-activated, cytoskeletal-degrading protease, was upregulated with aging and downregulated by FKBP1b (Table 3). This is the inverse pattern of that for cytoskeletal genes and suggests that calpain-1 upregulation might mediate important aspects of downregulation and degradation of the cytoskeleton during aging. Conversely, by downregulating calpain-1 expression, FKBP1b overexpression may restore or maintain neuronal structural integrity.

Efficacy and safety of long-term (LT) and short-term (ST) effects of FKBP1b overexpression

Another goal of the present study was to test whether long-term FKBP1b overexpression in mid-aged animals could prevent the emergence of cognitive impairment as effectively as short-term FKBP1b can reverse it (Gant et al., 2015). Results showed clearly that FKBP1b overexpression did not lose behavioral efficacy over extended time, as both long-term and short-term FKBP1b trea0tment groups substantially outperformed aged controls and performed similarly to each other and to young animals (Fig. 2). These results show cognitive impairment can be prevented by LT treatment beginning in mid-aged animals as well as reversed by ST treatment in aged animals.

An interesting question not addressed here is whether animals already performing at a high baseline, including young animals and the small percentage of aged animals that are unimpaired (e.g., Backman et al., 1996; Gallagher and Rapp, 1997; Tombaugh et al., 2002; Rowe et al., 2003; Rowe et al., 2007; Curlik et al., 2014; Menard et al., 2015) show improved memory with FKBP1b. It will be important in future studies to determine whether unimpaired animals are resistant or sensitive to the actions of FKBP1b on memory.

Relative to safety issues, FKBP1b expression was significantly higher in LT compared with ST rats (Fig. 3), indicating increased expression over the 9-month exposure or that expression is greater when initiated in mid-aged vs aged animals. Regardless, the health of LT rats appeared comparable to that of ST or age-matched vector control rats, as there was only one death and no apparent morbidity among LT rats over the 9-month course of the experiment. The clinical literature also indicates that AAV-mediated gene overexpression is generally long-lasting and safe in brain tissue, with extremely low probability of inducing oncogenic or other deleterious changes in DNA (Kaplitt et al., 2007; McCown, 2010).

Do normal-aging-induced cytoskeletal conditions model pre-neurofibrillary tangle pathology of AD?

589 Advanced age is the leading risk factor for AD (Reitz et al., 2011), suggesting that some
590 processes that drive normal brain aging also increase susceptibility to AD. Considerable
591 evidence indicates that Ca^{2+} dysregulation is present in both normal brain aging and AD (see
592 Introduction) and, therefore, is positioned to play a role in age-dependent susceptibility to AD.
593 Cytoskeletal dysfunction, in the form of neurofibrillary tangles, is one of the hallmarks of AD
594 pathology. It is correlated with synaptic degeneration and characterized by microtubule
595 rarefaction and hyperphosphorylation of the microtubule associated protein tau (Wisniewski and
596 Terry, 1973; Grundke-Iqbal et al., 1979; Masliah et al., 1991; Jicha et al., 1997; Serrano-Pozo et
597 al., 2011; Webster et al., 2014). Here, we found that hippocampal cytoskeletal gene expression
598 is downregulated with aging and, in parallel with cognitive function, is restored by FKBP1b, very
599 possibly via Ca^{2+} signaling pathways. Accordingly, although tangles are not generally present in
600 animal models of normal brain aging, we suggest that declining FKBP1b function and resulting
601 Ca^{2+} dysregulation during normal aging in animals recapitulate brain aging processes in humans
602 that subtly degrade the cytoskeleton and, in susceptible individuals, eventually result in
603 irreversible neurofibrillary tangles and AD.

604

605 **References**

606 Alberini CM, Kandel ER (2014) The regulation of transcription in memory consolidation. Cold
607 Spring Harb Perspect Biol 7:a021741.
608 Backman C, Rose GM, Hoffer BJ, Henry MA, Bartus RT, Friden P, Granholm AC (1996)
609 Systemic administration of a nerve growth factor conjugate reverses age-related
610 cognitive dysfunction and prevents cholinergic neuron atrophy. J Neurosci 16:5437-
611 5442.
612 Bartus RT, Dean RL, 3rd, Fleming DL (1979) Aging in the rhesus monkey: effects on visual
613 discrimination learning and reversal learning. J Gerontol 34:209-219.
614 Bezprozvanny I, Mattson MP (2008) Neuronal calcium mishandling and the pathogenesis of
615 Alzheimer's disease. Trends Neurosci 31:454-463.
616 Binder DK, Scharfman HE (2004) Brain-derived neurotrophic factor. Growth Factors 22:123-
617 131.

618 Bizon JL, LaSarge CL, Montgomery KS, McDermott AN, Setlow B, Griffith WH (2009) Spatial
619 reference and working memory across the lifespan of male Fischer 344 rats. Neurobiol
620 Aging 30:646-655.
621 Blalock EM, Geddes JW, Chen KC, Porter NM, Markesbery WR, Landfield PW (2004) Incipient
622 Alzheimer's disease: microarray correlation analyses reveal major transcriptional and
623 tumor suppressor responses. Proceedings of the National Academy of Sciences of the
624 United States of America 101:2173-2178.
625 Blalock EM, Chen KC, Sharrow K, Herman JP, Porter NM, Foster TC, Landfield PW (2003)
626 Gene microarrays in hippocampal aging: statistical profiling identifies novel processes
627 correlated with cognitive impairment. J Neurosci 23:3807-3819.
628 Blalock EM, Chen KC, Stromberg AJ, Norris CM, Kadish I, Kraner SD, Porter NM, Landfield PW
629 (2005) Harnessing the power of gene microarrays for the study of brain aging and
630 Alzheimer's disease: statistical reliability and functional correlation. Ageing Res Rev
631 4:481-512.
632 Bolstad BM, Irizarry RA, Astrand M, Speed TP (2003) A comparison of normalization methods
633 for high density oligonucleotide array data based on variance and bias. Bioinformatics
634 19:185-193.
635 Briz V, Baudry M (2016) Calpains: Master Regulators of Synaptic Plasticity. The Neuroscientist
636 23:221-231.
637 Chen KC, Blalock EM, Curran-Rauhut MA, Kadish I, Blalock SJ, Brewer L, Porter NM, Landfield
638 PW (2013) Glucocorticoid-dependent hippocampal transcriptome in male rats: pathway-
639 specific alterations with aging. Endocrinology 154:2807-2820.
640 Curlik DM, Weiss C, Nicholson DA, Disterhoft JF (2014) Age-related impairments on one
641 hippocampal-dependent task predict impairments on a subsequent hippocampal-
642 dependent task. Behav Neurosci 128:676-688.
643 Disterhoft JF, Thompson LT, Moyer JR, Jr., Mogul DJ (1996) Calcium-dependent
644 afterhyperpolarization and learning in young and aging hippocampus. Life Sci 59:413-
645 420.
646 Fletcher BR, Hill GS, Long JM, Gallagher M, Shapiro ML, Rapp PR (2014) A fine balance:
647 Regulation of hippocampal Arc/Arg3.1 transcription, translation and degradation in a rat
648 model of normal cognitive aging. Neurobiol Learn Mem 115:58-67.
649 Forster MJ, Lal H (1992) Within-subject behavioral analysis of recent memory in aging mice.
650 Behav Pharmacol 3:337-349.
651 Furman JL, Norris CM (2014) Calcineurin and glial signaling: neuroinflammation and beyond. J
652 Neuroinflammation 11:158.
653 Gall CM, Pinkstaff JK, Lauterborn JC, Xie Y, Lynch G (2003) Integrins regulate neuronal
654 neurotrophin gene expression through effects on voltage-sensitive calcium channels.
655 Neuroscience 118:925-940.
656 Gallagher M, Rapp PR (1997) The use of animal models to study the effects of aging on
657 cognition. Annu Rev Psychol 48:339-370.
658 Galvin JE, Ginsberg SD (2005) Expression profiling in the aging brain: a perspective. Ageing
659 Res Rev 4:529-547.
660 Gant JC, Chen KC, Kadish I, Blalock EM, Thibault O, Porter NM, Landfield PW (2015) Reversal
661 of Aging-Related Neuronal Ca2+ Dysregulation and Cognitive Impairment by Delivery of
662 a Transgene Encoding FK506-Binding Protein 12.6/1b to the Hippocampus. J Neurosci
663 35:10878-10887.
664 Gant JC, Chen KC, Norris CM, Kadish I, Thibault O, Blalock EM, Porter NM, Landfield PW
665 (2011) Disrupting function of FK506-binding protein 1b/12.6 induces the Ca(2)+-
666 dysregulation aging phenotype in hippocampal neurons. J Neurosci 31:1693-1703.

667 Gant JC, Blalock EM, Chen KC, Kadish I, Porter NM, Norris CM, Thibault O, Landfield PW
668 (2014) FK506-binding protein 1b/12.6: a key to aging-related hippocampal Ca2+
669 dysregulation? Eur J Pharmacol 739:74-82.
670 Gibson GE, Peterson C (1987) Calcium and the aging nervous system. Neurobiol Aging 8:329-
671 343.
672 Gibson GE, Zhang H, Toral-Barza L, Szolosi S, Tofel-Grehl B (1996) Calcium stores in cultured
673 fibroblasts and their changes with Alzheimer's disease. Biochim Biophys Acta 1316:71-
674 77.
675 Ginsberg SD, Mirnics K (2006) Functional genomic methodologies. Prog Brain Res 158:15-40.
676 Graef IA, Mermelstein PG, Stankunas K, Neilson JR, Deisseroth K, Tsien RW, Crabtree GR
677 (1999) L-type calcium channels and GSK-3 regulate the activity of NF-ATc4 in
678 hippocampal neurons. Nature 401:703-708.
679 Greer PL, Greenberg ME (2008) From synapse to nucleus: calcium-dependent gene
680 transcription in the control of synapse development and function. Neuron 59:846-860.
681 Grundke-Iqbal I, Johnson AB, Wisniewski HM, Terry RD, Iqbal K (1979) Evidence that
682 Alzheimer neurofibrillary tangles originate from neurotubules. Lancet 1:578-580.
683 Guzowski JF, Lyford GL, Stevenson GD, Houston FP, McGaugh JL, Worley PF, Barnes CA
684 (2000) Inhibition of activity-dependent arc protein expression in the rat hippocampus
685 impairs the maintenance of long-term potentiation and the consolidation of long-term
686 memory. J Neurosci 20:3993-4001.
687 Hemond P, Jaffe DB (2005) Caloric restriction prevents aging-associated changes in spike-
688 mediated Ca2+ accumulation and the slow afterhyperpolarization in hippocampal CA1
689 pyramidal neurons. Neuroscience 135:413-420.
690 Hoeffer CA, Tang W, Wong H, Santillan A, Patterson RJ, Martinez LA, Tejada-Simon MV,
691 Paylor R, Hamilton SL, Klann E (2008) Removal of FKBP12 enhances mTOR-Raptor
692 interactions, LTP, memory, and perseverative/repetitive behavior. Neuron 60:832-845.
693 Huang DW, Sherman BT, Tan Q, Collins JR, Alvord WG, Roayaei J, Stephens R, Baseler MW,
694 Lane HC, Lempicki RA (2007) The DAVID Gene Functional Classification Tool: a novel
695 biological module-centric algorithm to functionally analyze large gene lists. Genome Biol
696 8:R183.
697 Huang W, Sherman BT, Lempicki RA (2009) Systematic and integrative analysis of large gene
698 lists using DAVID bioinformatics resources. Nat Protoc 4:44-57.
699 Jicha GA, Lane E, Vincent I, Otvos L, Jr., Hoffmann R, Davies P (1997) A conformation- and
700 phosphorylation-dependent antibody recognizing the paired helical filaments of
701 Alzheimer's disease. J Neurochem 69:2087-2095.
702 Johnson SC, Rabinovitch PS, Kaeberlein M (2013) mTOR is a key modulator of ageing and
703 age-related disease. Nature 493:338-345.
704 Kadish I, Van Groen T (2003) Differences in lesion-induced hippocampal plasticity between
705 mice and rats. Neuroscience 116:499-509.
706 Kadish I, Thibault O, Blalock EM, Chen KC, Gant JC, Porter NM, Landfield PW (2009)
707 Hippocampal and cognitive aging across the lifespan: a bioenergetic shift precedes and
708 increased cholesterol trafficking parallels memory impairment. J Neurosci 29:1805-1816.
709 Kang CB, Hong Y, Dhe-Paganon S, Yoon HS (2008) FKBP family proteins: immunophilins with
710 versatile biological functions. Neurosignals 16:318-325.
711 Kaplitt MG, Feigin A, Tang C, Fitzsimons HL, Mattis P, Lawlor PA, Bland RJ, Young D, Strybing
712 K, Eidelberg D, During MJ (2007) Safety and tolerability of gene therapy with an adeno-
713 associated virus (AAV) borne GAD gene for Parkinson's disease: an open label, phase I
714 trial. Lancet 369:2097-2105.
715 Khachaturian ZS (1989) The role of calcium regulation in brain aging: reexamination of a
716 hypothesis. Aging (Milano) 1:17-34.

717 Kuchibhotla KV, Goldman ST, Lattarulo CR, Wu HY, Hyman BT, Bacskai BJ (2008) Abeta
718 plaques lead to aberrant regulation of calcium homeostasis in vivo resulting in structural
719 and functional disruption of neuronal networks. Neuron 59:214-225.
720 Landfield PW (1987) 'Increased calcium-current' hypothesis of brain aging. Neurobiol Aging
721 8:346-347.
722 Landfield PW, Pitler TA (1984) Prolonged Ca2+-dependent afterhyperpolarizations in
723 hippocampal neurons of aged rats. Science 226:1089-1092.
724 Latimer CS, Brewer LD, Searcy JL, Chen KC, Popovic J, Kraner SD, Thibault O, Blalock EM,
725 Landfield PW, Porter NM (2014) Vitamin D prevents cognitive decline and enhances
726 hippocampal synaptic function in aging rats. Proc Natl Acad Sci U S A 111:E4359-4366.
727 Lee YS, Silva AJ (2009) The molecular and cellular biology of enhanced cognition. Nat Rev
728 Neurosci 10:126-140.
729 Lehnart SE, Mongillo M, Bellinger A, Lindegger N, Chen BX, Hsueh W, Reiken S, Wronska A,
730 Drew LJ, Ward CW, Lederer WJ, Kass RS, Morley G, Marks AR (2008) Leaky Ca2+
731 release channel/ryanodine receptor 2 causes seizures and sudden cardiac death in
732 mice. J Clin Invest 118:2230-2245.
733 Liu X, Betzenhauser MJ, Reiken S, Meli AC, Xie W, Chen BX, Arancio O, Marks AR (2012) Role
734 of leaky neuronal ryanodine receptors in stress-induced cognitive dysfunction. Cell
735 150:1055-1067.
736 Luebke JI, Amatrudo JM (2012) Age-related increase of sI(AHP) in prefrontal pyramidal cells of
737 monkeys: relationship to cognition. Neurobiol Aging 33:1085-1095.
738 Lynch G, Baudry M (1987) Brain spectrin, calpain and long-term changes in synaptic efficacy.
739 Brain Res Bull 18:809-815.
740 Lynch G, Rex CS, Chen LY, Gall CM (2008) The substrates of memory: defects, treatments,
741 and enhancement. Eur J Pharmacol 585:2-13.
742 MacMillan D, McCarron JG (2009) Regulation by FK506 and rapamycin of Ca2+ release from
743 the sarcoplasmic reticulum in vascular smooth muscle: the role of FK506 binding
744 proteins and mTOR. Br J Pharmacol 158:1112-1120.
745 Markowska AL (1999) Sex dimorphisms in the rate of age-related decline in spatial memory:
746 relevance to alterations in the estrous cycle. J Neurosci 19:8122-8133.
747 Masliah E, Hansen L, Albright T, Mallory M, Terry RD (1991) Immunoelectron microscopic study
748 of synaptic pathology in Alzheimer's disease. Acta Neuropathol 81:428-433.
749 McCown TJ (2010) The future of epilepsy treatment: focus on adeno-associated virus vector
750 gene therapy. Drug News Perspect 23:281-286.
751 Menard C, Quirion R, Vigneault E, Bouchard S, Ferland G, El Mestikawy S, Gaudreau P (2015)
752 Glutamate presynaptic vesicular transporter and postsynaptic receptor levels correlate
753 with spatial memory status in aging rat models. Neurobiol Aging 36:1471-1482.
754 Michaelis ML, Johe K, Kitos TE (1984) Age-dependent alterations in synaptic membrane
755 systems for Ca2+ regulation. Mech Ageing Dev 25:215-225.
756 Murchison D, Griffith WH (2007) Calcium buffering systems and calcium signaling in aged rat
757 basal forebrain neurons. Aging Cell 6:297-305.
758 Murphy GG, Shah V, Hell JW, Silva AJ (2006) Investigation of age-related cognitive decline
759 using mice as a model system: neurophysiological correlates. Am J Geriatr Psychiatry
760 14:1012-1021.
761 Nixon RA, Saito KI, Grynspan F, Griffin WR, Katayama S, Honda T, Mohan PS, Shea TB,
762 Beermann M (1994) Calcium-activated neutral proteinase (calpain) system in aging and
763 Alzheimer's disease. Ann N Y Acad Sci 747:77-91.
764 Oh MM, Oliveira FA, Disterhoft JF (2010) Learning and aging related changes in intrinsic
765 neuronal excitability. Front Aging Neurosci 2:2.

766 Overk C, Masliah E (2017) Perspective on the calcium dyshomeostasis hypothesis in the
767 pathogenesis of selective neuronal degeneration in animal models of Alzheimer's
768 disease. Alzheimers Dement 13:183-185.
769 Ploski JE, Pierre VJ, Smucny J, Park K, Monsey MS, Overeem KA, Schafe GE (2008) The
770 activity-regulated cytoskeletal-associated protein (Arc/Arg3.1) is required for memory
771 consolidation of pavlovian fear conditioning in the lateral amygdala. J Neurosci
772 28:12383-12395.
773 Reitz C, Brayne C, Mayeux R (2011) Epidemiology of Alzheimer disease. Nat Rev Neurol
774 7:137-152.
775 Reynolds JN, Carlen PL (1989) Diminished calcium currents in aged hippocampal dentate gyrus
776 granule neurones. Brain Res 479:384-390.
777 Rowe WB, O'Donnell JP, Pearson D, Rose GM, Meaney MJ, Quirion R (2003) Long-term
778 effects of BIBN-99, a selective muscarinic M2 receptor antagonist, on improving spatial
779 memory performance in aged cognitively impaired rats. Behav Brain Res 145:171-178.
780 Rowe WB, Blalock EM, Chen KC, Kadish I, Wang D, Barrett JE, Thibault O, Porter NM, Rose
781 GM, Landfield PW (2007) Hippocampal expression analyses reveal selective association
782 of immediate-early, neuroenergetic, and myelinogenic pathways with cognitive
783 impairment in aged rats. J Neurosci 27:3098-3110.
784 Rozkalne A, Hyman BT, Spires-Jones TL (2011) Calcineurin inhibition with FK506 ameliorates
785 dendritic spine density deficits in plaque-bearing Alzheimer model mice. Neurobiol Dis
786 41:650-654.
787 Schafe GE, LeDoux JE (2000) Memory consolidation of auditory pavlovian fear conditioning
788 requires protein synthesis and protein kinase A in the amygdala. J Neurosci 20:RC96.
789 Scharfman HE, Schwartzkroin PA (1989) Protection of dentate hilar cells from prolonged
790 stimulation by intracellular calcium chelation. Science 246:257-260.
791 Scheinert RB, Asokan A, Rani A, Kumar A, Foster TC, Ormerod BK (2015) Some hormone,
792 cytokine and chemokine levels that change across lifespan vary by cognitive status in
793 male Fischer 344 rats. Brain Behav Immun 49:216-232.
794 Searcy JL, Phelps JT, Pancani T, Kadish I, Popovic J, Anderson KL, Beckett TL, Murphy MP,
795 Chen KC, Blalock EM, Landfield PW, Porter NM, Thibault O (2012) Long-term
796 pioglitazone treatment improves learning and attenuates pathological markers in a
797 mouse model of Alzheimer's disease. J Alzheimers Dis 30:943-961.
798 Serrano-Pozo A, Frosch MP, Masliah E, Hyman BT (2011) Neuropathological alterations in
799 Alzheimer disease. Cold Spring Harb Perspect Med 1:a006189.
800 Stephens DN, Weidmann R, Quartermain D, Sarter M (1985) Reversal learning in senescent
801 rats. Behav Brain Res 17:193-202.
802 Steward O, Wallace CS, Lyford GL, Worley PF (1998) Synaptic activation causes the mRNA for
803 the IEG Arc to localize selectively near activated postsynaptic sites on dendrites. Neuron
804 21:741-751.
805 Stutzmann GE, Smith I, Caccamo A, Oddo S, Laferla FM, Parker I (2006) Enhanced ryanodine
806 receptor recruitment contributes to Ca2+ disruptions in young, adult, and aged
807 Alzheimer's disease mice. J Neurosci 26:5180-5189.
808 Thibault O, Landfield PW (1996) Increase in single L-type calcium channels in hippocampal
809 neurons during aging. Science 272:1017-1020.
810 Thibault O, Gant JC, Landfield PW (2007) Expansion of the calcium hypothesis of brain aging
811 and Alzheimer's disease: minding the store. Aging Cell 6:307-317.
812 Thompson LT, Moyer JR, Jr., Disterhoft JF (1996) Trace eyeblink conditioning in rabbits
813 demonstrates heterogeneity of learning ability both between and within age groups.
814 Neurobiol Aging 17:619-629.

Tombaugh GC, Rowe WB, Rose GM (2005) The slow afterhyperpolarization in hippocampal CA1 neurons covaries with spatial learning ability in aged Fisher 344 rats. J Neurosci 25:2609-2616.

Tombaugh GC, Rowe WB, Chow AR, Michael TH, Rose GM (2002) Theta-frequency synaptic potentiation in CA1 in vitro distinguishes cognitively impaired from unimpaired aged Fischer 344 rats. J Neurosci 22:9932-9940.

VanGuilder HD, Bixler GV, Brucklacher RM, Farley JA, Yan H, Warrington JP, Sonntag WE, Freeman WM (2011) Concurrent hippocampal induction of MHC II pathway components and glial activation with advanced aging is not correlated with cognitive impairment. J Neuroinflammation 8:138.

Verkhratsky A, Toescu EC (1998) Calcium and neuronal ageing. Trends Neurosci 21:2-7.

Webster SJ, Bachstetter AD, Nelson PT, Schmitt FA, Van Eldik LJ (2014) Using mice to model Alzheimer's dementia: an overview of the clinical disease and the preclinical behavioral changes in 10 mouse models. Front Genet 5:88.

Weindruch R, Prolla TA (2002) Gene expression profile of the aging brain. Arch Neurol 59:1712-1714.

Wisniewski HM, Terry RD (1973) Morphology of the aging brain, human and animal. Prog Brain Res 40:167-186.

Wyss JM, Chambless BD, Kadish I, van Groen T (2000) Age-related decline in water maze learning and memory in rats: strain differences. Neurobiol Aging 21:671-681.

Zalk R, Lehnart SE, Marks AR (2007) Modulation of the ryanodine receptor and intracellular calcium. Annu Rev Biochem 76:367-385.

840 **Figure Legends**

841 Figure 1: Experimental Design: To compare long-term with short-term exposure to FKBP1b
842 overexpression, aging rats were bilaterally injected in the hippocampus with AAV-FKBP1b at
843 two different ages, one group at 13 months-old (long-term) and one group at 19-months-old
844 (short-term) (small, vertical arrows). A third group received control vector (AAV-eGFP) at 13
845 months-old and a young control group received no injections. All animals were tested for spatial
846 learning in the Morris water maze (MWM), 3 aged groups at 21 months of age, and 1 young
847 control group at 6-months of age (total N = 52). Animals were killed following MWM testing and
848 the mRNA from the dorsal hippocampus of one hemisphere was prepared for qPCR and
849 microarray analyses while the other hemisphere was post-fixed for immunohistochemistry (IHC).

850

851 Figure 2. Both long-term and short-term FKBP1b overexpression countered age-related decline
852 in spatial memory. (A) Reference Memory Probe. FKBP1b treatments countered age-related
853 deficits in reference memory probe performance. (B) Reversal Memory Probe. FKBP1b
854 treatments countered age-related deficits in the reversal memory probe trial. (C) Cued Testing.
855 With visual cues prominently highlighting location of the escape platform, no group differences
856 were found, indicating that memory test results were not due to differences in locomotor and/or
857 visual abilities. (* $p \leq 0.05$; ** $p \leq 0.01$; *** $p \leq 0.001$; **** $p \leq 0.0001$ significant pairwise contrast vs.
858 Aged Ctrl)

859

860 Figure 3. Hippocampal FKBP1b mRNA and protein levels were increased substantially by long-
861 term AAV-FKBP1b overexpression. Top: rtPCR quantification of Hippocampal Fkbp1b mRNA
862 expression (Fkbp1b / Gapdh) for each treatment group (one-way ANOVA on ranks, $p =$
863 0.000050; for pairwise contrast vs. Aged Ctrl; * $p \leq 0.05$; *** $p \leq 0.001$). Lower: Immunostaining

for hippocampal FKBP1b expression. Representative photomicrographs from (A) young control, (B) aged control, (C) aged short-term FKBP1b and (D) aged long-term FKBP1b. Note the substantial increase in FKBP1b expression at both the mRNA and protein levels, particularly in the LT-FKBP1b group. (sp- stratum pyramidale; DG- dentate gyrus; calbar- 500 uM)

Figure 4. Microarray Analysis Flowchart: effects of aging and FKBP1b on hippocampal gene transcription. Left: Total gene probe sets (29,218) were filtered to remove absent (low signal intensity) and incompletely annotated probe sets. Remaining genes (14,828) were tested by ANOVA ($p \leq 0.05$) followed by pairwise comparison (Fischer's pLSD, ≤ 0.05 between young control and aged control) to define aging-dependent genes. Right: Statistical template algorithm. Aging-dependent genes were categorized based on whether FKBP1b had no effect (I, III) or significantly countered aging's effect (II, IV). 99.8%) of Aging-dependent genes were assigned to a template based on criteria (described in text). A Monte Carlo simulation (1000 iterations, see Results) was used to estimate the number of genes expected in each template by chance. The number of genes assigned to each template in the observed data was significantly greater than the number expected by chance ($p \leq 0.0001$; binomial test; >11 fold increase for all templates). For extended data see Figure 4-1.

Figure 5. FKBP1b counters age-related decrease in hippocampal MAP2 protein expression. Top: semi-quantitative measures of MAP2 immunohistochemical staining densities are plotted as a function of treatment. Statistical analysis revealed a significant effect ($p = 0.0015$; one-way ANOVA) with a significant decrease from young control to aged control that was countered by long-term (LT) FKPB1b (** $p \leq 0.01$, *** $p \leq 0.001$, † n.s. trend $p = 0.06$; post-hoc Fisher's pLSD vs. Aged Control) . Lower: Immunostaining for hippocampal MAP2 expression. Representative

888 photomicrographs from (A) young control- rectangle defines region of quantitation, (B) aged
889 control, (C) aged short-term FKBP1b and (D) aged long-term FKBP1b. (calbar- 500 uM).

890

891 Table 1: Functional Categories overrepresented by genes assigned to the four expression
892 templates reflecting aging +/- FKBP1b-sensitivity. Shown are Gene Ontology Category
893 Annotations overrepresented by genes exhibiting expression patterns matching one of the four
894 templates (Fig. 4) in direction of change and sensitivity to FKBP1b, listed in order of
895 significance. Left: Aging effect unchanged by FKBP1b. Right: Aging effect countered (opposite
896 direction change) by FKBP1b. (#- number significant genes in category; p-value- modified
897 Fisher's exact test/ EASE score). For extended data see Table 1-1.

898

899 Table 2: FKBP1b counters age-related downregulation of cytoskeletal gene expression. Gene
900 symbols, descriptions, mean expression level (± SEM) per group, and one-way Analysis of
901 Variance (ANOVA) p-values are reported. Genes shown are the 39 cytoskeletal category genes
902 identified in Table 1 (template II) that were significantly downregulated with aging and
903 upregulated by FKBP1b treatment.

904

905 Table 3: FKBP1b counters age-related gene expression changes in key calcium signaling
906 pathways. Gene symbols, descriptions, mean expression level (± SEM) per group, and one-way
907 Analysis of Variance (ANOVA) p-values are reported. Genes presented are associated in the
908 Gene Ontology with calcium-related pathways, and are significantly altered with aging and
909 countered by FKBP1b treatment.

910

911 Figure 4-1: List of all significant genes ($p \leq 0.05$, one way ANOVA) and the mean (±SEM) signal
912 intensity values for each gene across groups, followed by ANOVA p-value. Pairwise contrast
913 (Fisher's pLSD) results color coded for significance (0. white- n.s., 1. red- upregulated, -1. blue-
914 downregulated). Page 1- Aging up, Unchanged by FK; page 23- Aging down, unchanged by FK;
915 page 46- Aging up, Down by FK; page 61- Aging down, Up by FK; page 74- Unchanged by
916 Aging

917

918 Table 1-1: Individual genes assigned to each of the functional categories that are listed in Table
919 1. Functional categories are grouped by template (I-IV) assignment and listed in order of
920 significance within template. In addition to listing the pathway name (Gene Ontology
921 Annotations), number of genes (#), and overrepresentation p-value (p-value: DAVID modified
922 Fisher's exact test/ EASE score), the individual aging-significant genes assigned to each
923 pathway are also listed (and hyperlinked to www.genecards.org for additional information)
924 alphabetically to the right of each p-value. reflecting aging +/- FKBP1b-sensitivity are shown.
925 Left: Aging effect unchanged by FKBP1b. Right: Aging effect countered (opposite direction
926 change) by FKBP1b. (#- number significant genes in category; p-value- modified Fisher's exact
927 test/ EASE score), followed by list of gene symbols associated with that over-represented
928 functional category for that template.

929

930

931

932

933

934

935

936

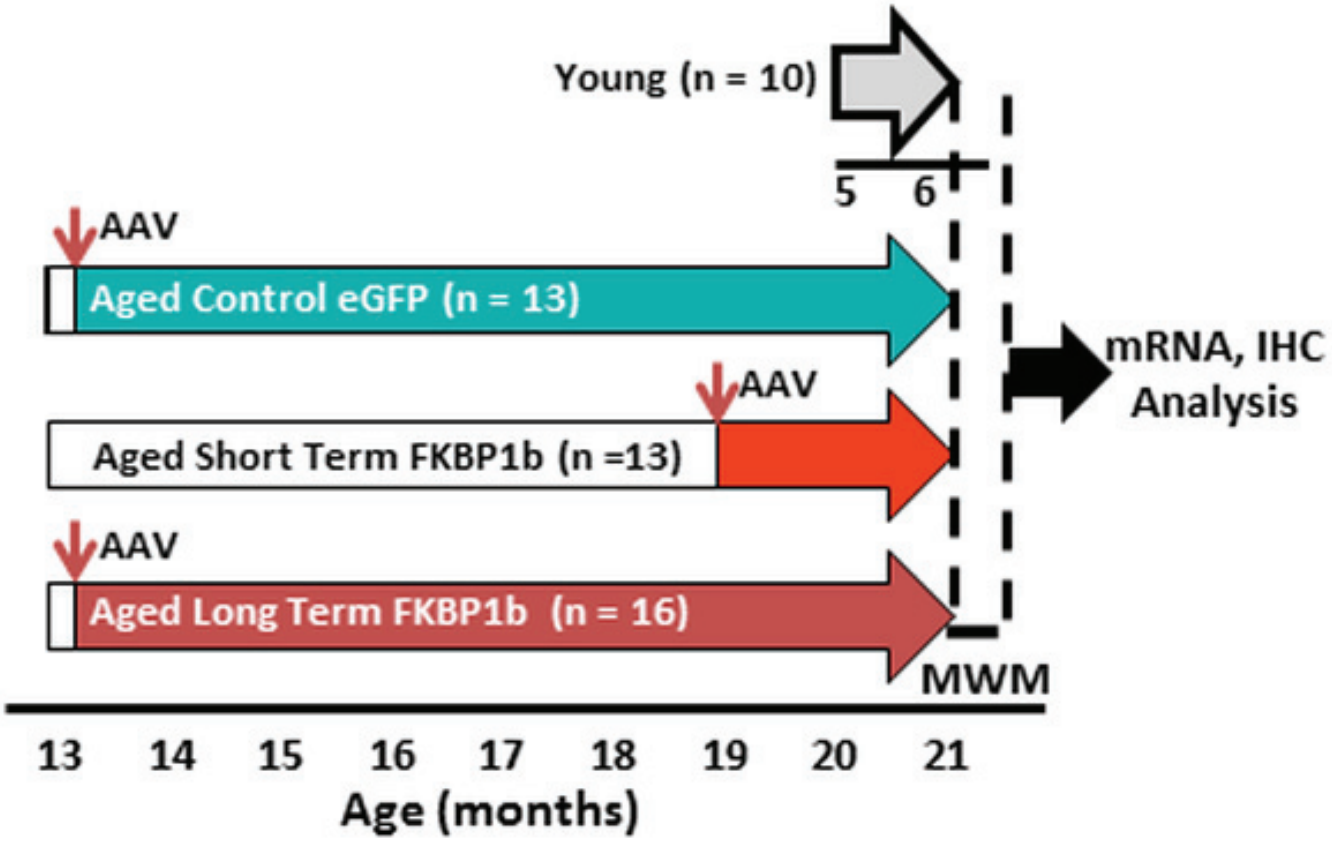

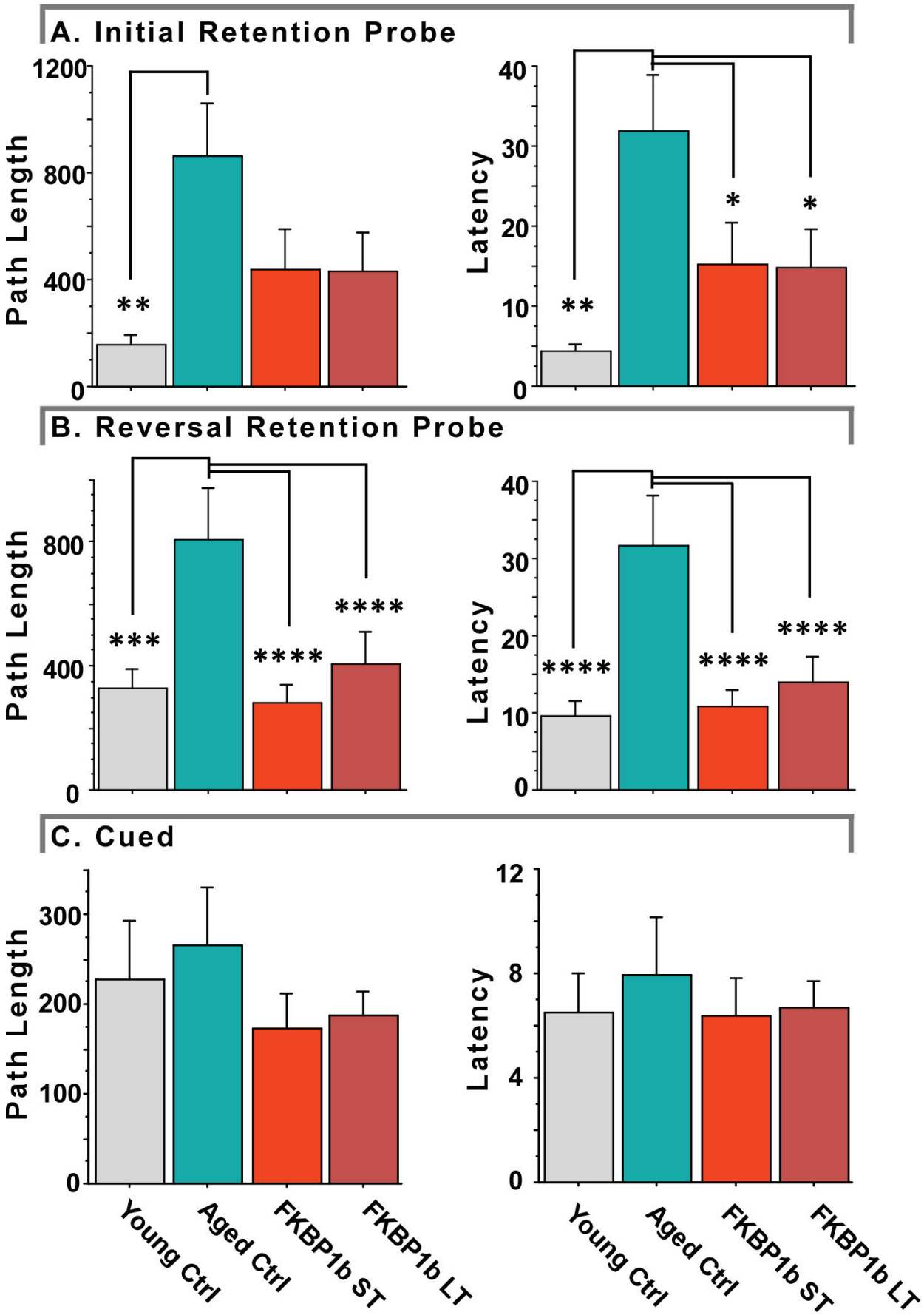

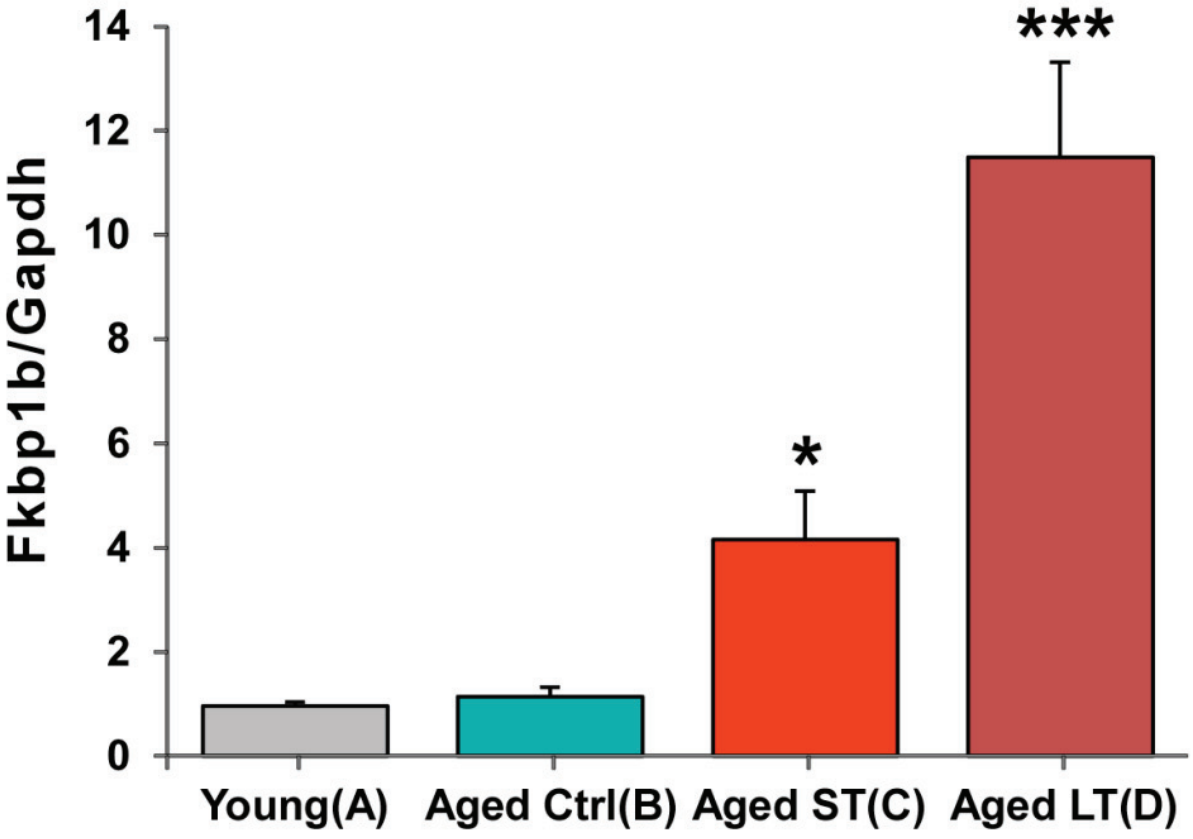

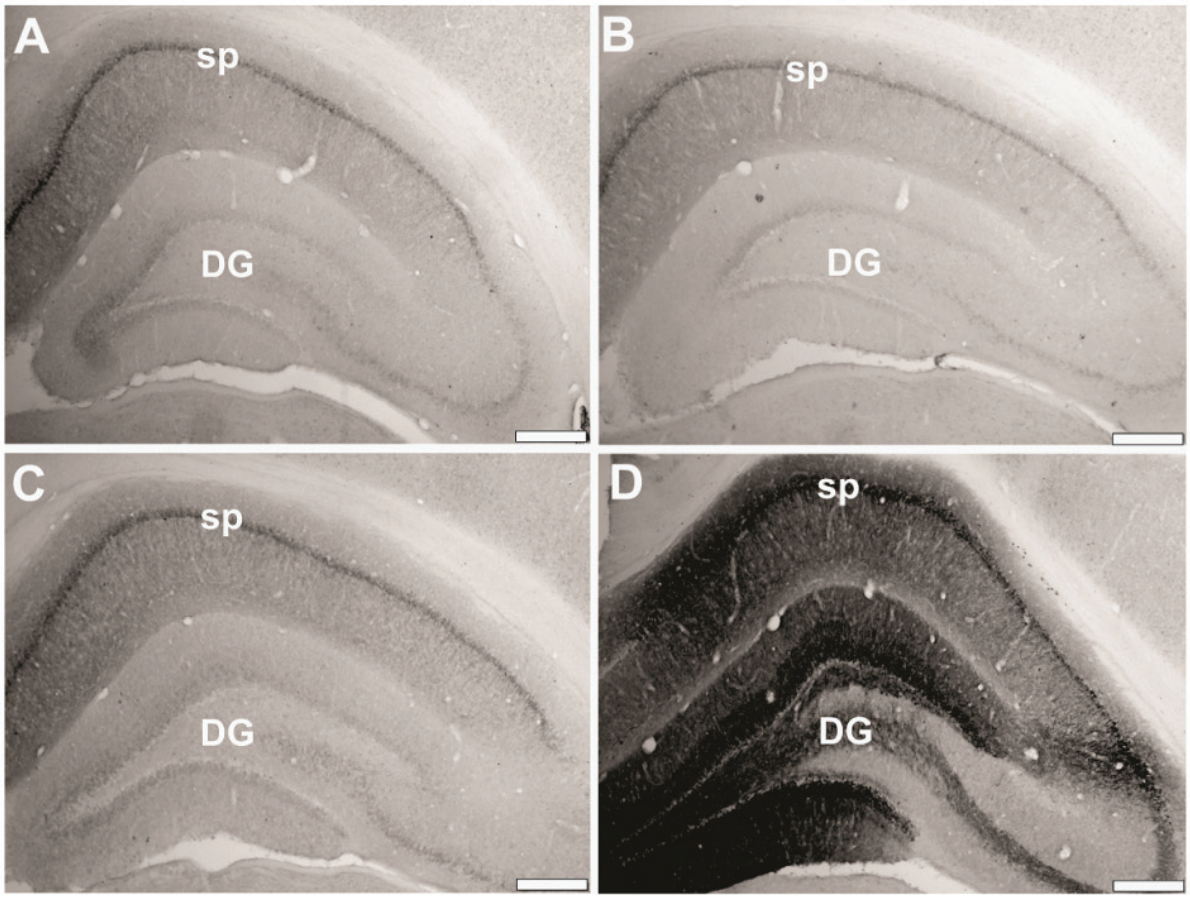

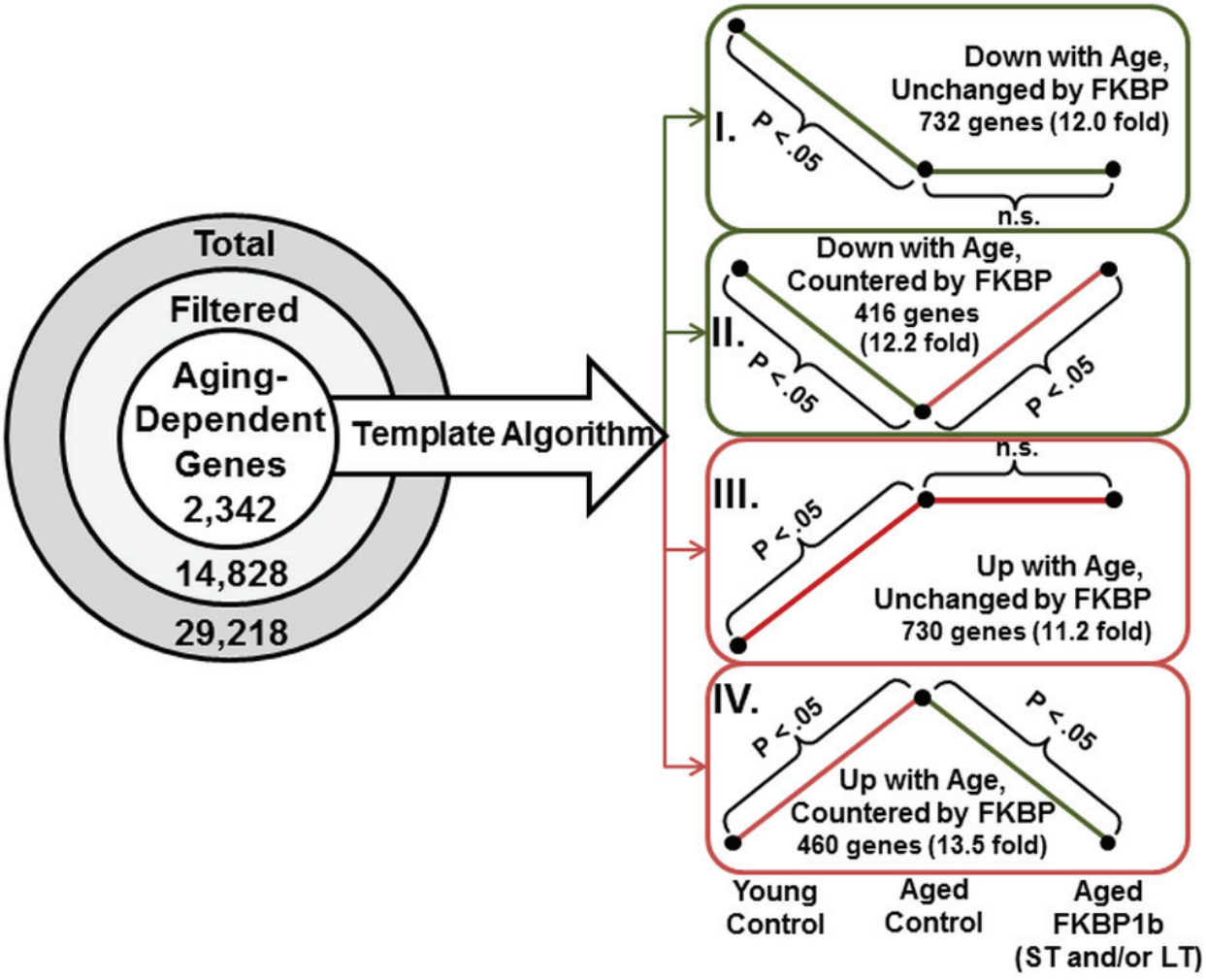

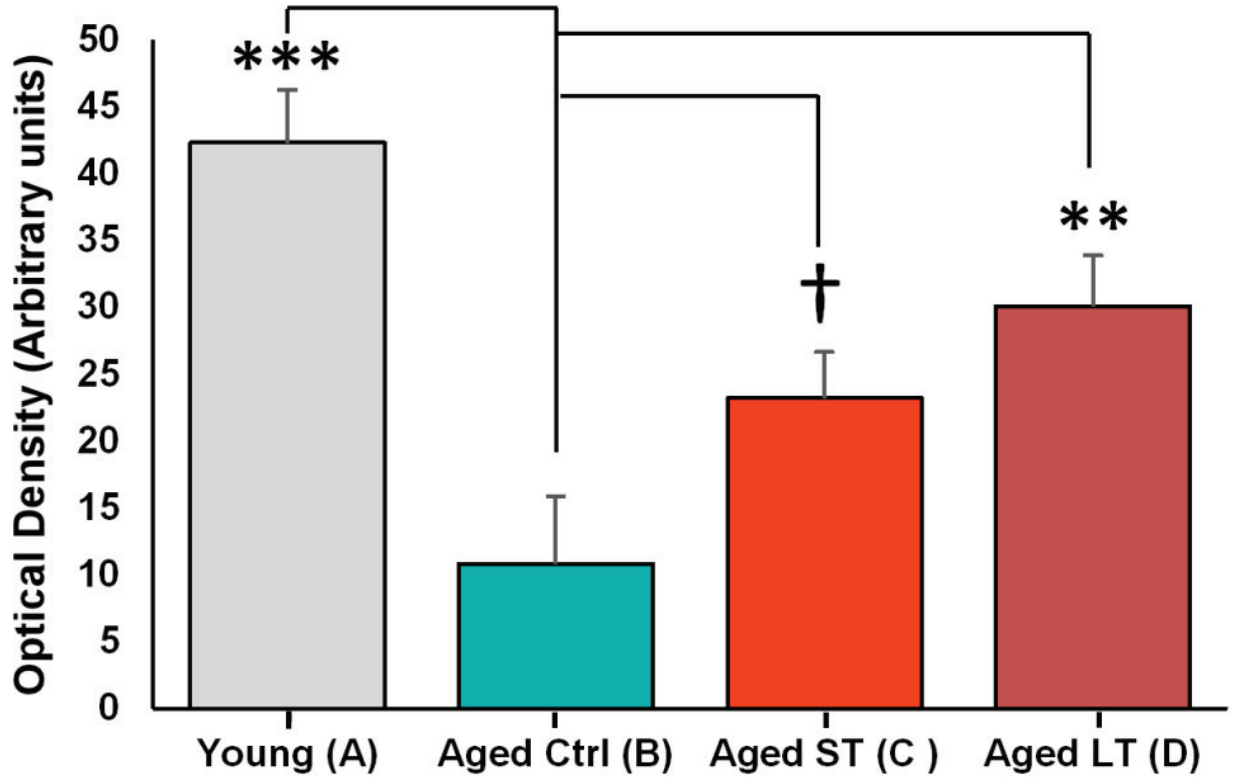

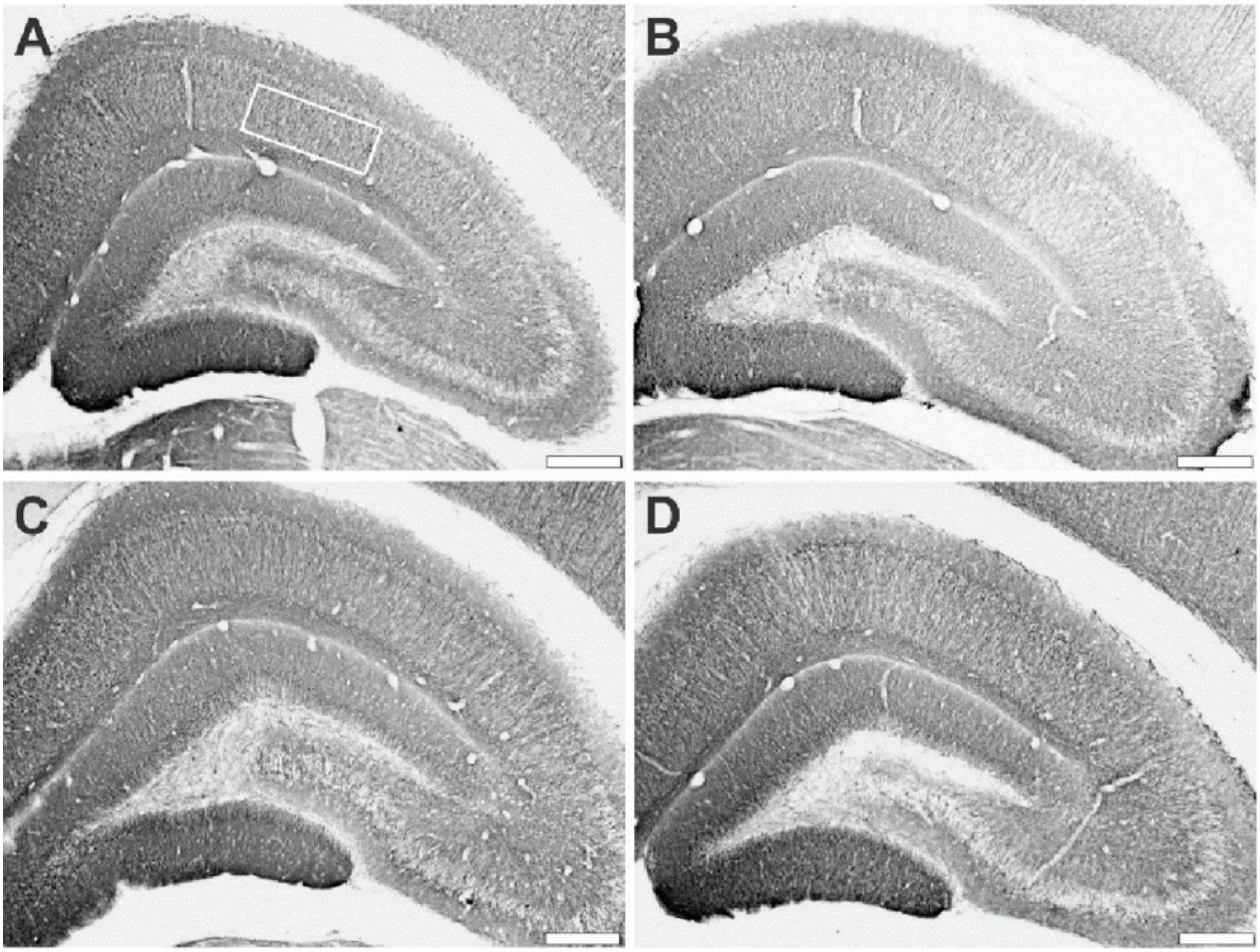

Table 1: Functional Categories overrepresented by genes assigned to the four expression templates reflecting aging +/- FKBP1b-sensitivity

I. Down with Age, Unchanged by FKBP1b	#	p-value
serine hydrolase activity	18	0.0019
cellular amino acid derivative biosynthesis	9	0.0029
integral to plasma membrane	27	0.0050
amine metabolic process	27	0.0082
tissue morphogenesis	19	0.0150
positive regulation of gene expression	36	0.0341

II. Down with Age, Up by FKBP1b	#	p-value
cytoskeleton	39	9.6E-04
passive transmembrane transporter activity	19	0.0039
extracellular region	41	0.0080
ectoderm development	8	0.0249
regulation of actin cytoskeleton	6	0.0265
metalloendopeptidase activity	6	0.0335
regulation of MAP kinase activity	8	0.0387

III. Up with Age, Unchanged by FKBP1b	#	p-value
translational elongation	36	5.9E-23
lysosome	35	2.7E-13
immune system process	76	5.0E-11
endosomal part	12	3.4E-06
immune effector process	21	3.7E-06
ribosomal small subunit biogenesis	7	2.0E-05
leukocyte activity during immune response	11	2.3E-05
antigen processing and presentation	15	4.0E-05
response to stress	97	7.3E-05
T cell activation	15	0.0010
regulation of acute inflammatory response	8	0.0020
protein kinase cascade	26	0.0036
carbohydrate binding	25	0.0045
protein amino acid phosphorylation	44	0.0056
response to oxidative stress	18	0.0095
response to lipid	7	0.0134

IV. Up with Age, Down by FKBP1b	#	p-value
extracellular matrix	20	1.0E-04
primary transmemb. transporter activity	11	9.1E-04
regulation of cell motion	15	0.0010
basolateral plasma membrane	15	0.0021
Golgi cisterna	6	0.0027
blood vessel development	16	0.0035
membrane-bounded vesicle	29	0.0076
response to oxygen levels	13	0.0162
response to estrogen stimulus	10	0.0246
membrane organization	16	0.0247
intracellular transport	23	0.0281
organelle membrane	39	0.0385
homeostasis of number of cells	8	0.0419

cell-cell adhesion	17	0.0324

Table 2: FKBP1b counters age-related downregulation of cytoskeletal gene expression

Gene	Description	Young Control	Aged Control	Short- Term (ST)	Long- Term (LT)	ANOVA p-value
Actr1a	ARP1 actin-related prot.1 homolog A	843±10	753±18	811±15	801±15	0.0046
Add1	adducin 1 (alpha)	2156±15	2051±38	2155±20	2061±24	0.0096
Arl8b	ADP-ribosylation factor-like 8B	3935±28	3603±86	3778±43	3817±40	0.0037
Calm2	calmodulin 2	8691±58	8281±104	8606±33	8449±69	0.0037
Ccdc99	coiled-coil domain containing 99	91±2	77±1	90±3	81±2	0.0007
Cort	cortistatin	296±2	272±8	274±5	294±5	0.0068
Csrp3	cysteine and glycine-rich protein 3	54±1	43±2	47±2	51±2	0.001
Csta	cystatin A (stefin A)	105±4	84±2	95±4	104±7	0.0181
Dnai2	dynein, axonemal, intermediate chain 2	80±2	70±4	73±2	81±3	0.0311
Emd	emerin	752±5	707±10	739±9	708±8	0.0015
Gphn	gephyrin	839±10	774±28	847±8	810±14	0.0296
Kb23	type II keratin Kb23	301±8	175±10	228±28	253±23	0.0027
Kifap3	kinesin-associated protein 3	2442±26	2264±23	2373±24	2366±20	0.0007
Krt10	keratin 10	73±3	59±2	61±2	73±5	0.0127
Krt17	keratin 17	65±2	53±2	62±2	67±2	0.0012
Krt23	keratin 23 (histone deacetylase inducible)	59±2	52±1	55±2	61±2	0.0117
Krt24	keratin 24	55±1	47±1	51±1	51±1	0.0014
Krt28	keratin 28	99±3	87±3	86±2	101±4	0.0037
Krt33b	keratin 33B	166±9	122±4	137±8	164±11	0.0064
Krt9	keratin 9	153±3	121±4	123±4	149±4	6.0E-06
Krtap1-5	keratin associated protein 1-5	66±3	55±3	58±0	64±1	0.0174
Lmnb2	lamin B2	121±1	111±3	118±2	123±3	0.0238
Mk1	Mk1 protein	61±2	51±2	59±1	54±3	0.0176
Myoz3	myozenin 3	359±2	336±8	359±6	357±6	0.0478
Pfn2	profilin 2	3277±33	2970±63	3134±33	3138±24	0.0006
Pja2	praja ring finger 2	4192±50	3998±53	4203±26	4060±13	0.0037
Ppp2ca	protein phosphatase 2 alpha	4039±35	3762±46	3946±15	3929±24	0.0001

Ppp4c	protein phosphatase 4, catalytic subunit	739±13	648±32	689±12	742±11	0.0063
Prph	peripherin	96±3	82±2	87±2	95±5	0.0309
Sec62	SEC62 homolog (S. cerevisiae)	1106±9	1044±6	1095±19	1085±14	0.031
Sept4	septin 4	2445±66	2035±145	2392±77	2371±68	0.0313
Sept7	septin 7	2249±25	2123±40	2288±28	2279±36	0.0115
Shroom4	shroom family member 4	141±2	115±5	126±5	136±6	0.0138
Tmem200a	transmembrane protein 200A	2344±36	2001±46	2072±50	2303±29	2.0E-05
Tns4	tensin 4	64±1	56±2	60±1	66±2	0.0008
Trim32	tripartite motif-containing 32	1640±15	1482±23	1494±36	1608±28	0.0009
Trip10	thyroid hormone receptor interactor 10	252±6	224±7	241±8	261±8	0.0158
Tuba1c	tubulin, alpha 1C	2354±28	2131±27	2150±43	2309±33	0.0003
Ywhaz	tyrosine 3/5-monooxygenase zeta	5666±36	5491±47	5655±38	5506±37	0.0074

Table 3: FKBP1b counters age-related gene expression changes in key calcium signaling pathways.

Name		Young Control	Aged Control	Short Term (ST)	Long Term (LT)	ANOVA p-value
Cab39	calcium binding protein 39	1499 ± 15	1387 ± 30	1483 ± 16	1469 ± 19	0.0074
Cabp4	calcium binding protein 4	193 ± 02	162 ± 07	170 ± 07	181 ± 04	0.0034
Calm2	calmodulin 2	8691 ± 58	8281 ± 104	8606 ± 33	8449 ± 69	0.0037
Calpns1	calpain, small subunit 1	2910 ± 18	2755 ± 28	2929 ± 24	2838 ± 55	0.0129
Ppp3cb	protein phosphatase 3 (calcineurin), catalytic subunit, beta	3295 ± 36	2942 ± 72	3054 ± 41	3198 ± 53	0.0009
	Upregulated with age, Downregulated by FKBP1b					
Camk1	calcium/calmodulin-dependent protein kinase I	231 ± 04	262 ± 11	238 ± 06	226 ± 04	0.0089
Capn1	calpain 1, large subunit	191 ± 04	206 ± 04	198 ± 04	186 ± 02	0.0080
Cib1	calcium and integrin binding 1 (calmyrin)	145 ± 03	173 ± 03	164 ± 03	156 ± 06	0.0012
Orai1	ORAI calcium release-activated calcium modulator 1	264 ± 04	279 ± 05	263 ± 03	270 ± 03	0.0389
S100a11	S100 calcium binding protein A11 (calgizzarin)	205 ± 11	329 ± 40	221 ± 13	228 ± 15	0.0049
S100a6	S100 calcium binding protein A6	95 ± 02	114 ± 05	103 ± 02	105 ± 01	0.0018